

“The functional characterization of mammalian non-coding Y RNAs”

Dissertation

zur Erlangung des
Doktorgrades der Naturwissenschaften (Dr. rer. nat.)
der

Naturwissenschaftlichen Fakultät I – Biowissenschaften –
der Martin-Luther-Universität
Halle-Wittenberg,

vorgelegt

von Herrn Marcel Köhn

geb. am 04.01.1983 in Wolgast

Öffentlich verteidigt am 30.10.2015

Gutachter:

Prof. Dr. Stefan Hüttelmaier (Halle, Deutschland)

Prof. Dr. Elmar Wahle (Halle, Deutschland)

Prof. Dr. Daniel Zenklusen (Montreal, Kanada)

Contents

Abstract

1. Non-coding RNAs (ncRNAs)

2. NcRNA synthesis by RNA polymerase III

2.1. *NcRNAs transcribed from type I and II POLIII-genes*

2.2. *NcRNAs transcribed from type III POLIII-genes*

3. The non-coding Y RNAs

3.1. *Evolution of Y RNAs*

3.2. *Y RNA genes and expression patterns*

3.3. *Processing of Y RNAs*

3.4. *Subcellular localization of Y RNAs*

3.5. *Y RNA-associated proteins*

3.6. *The Y RNA core proteins – La and Ro60*

3.7. *A paradigm of accessory Y RNA-binding proteins – IGF2BPs*

3.8. *The characterization of Y RNPs*

3.9. *The association of Y3/Y3** with mRNA 3'-end processing factors*

4. Y RNA functions

4.1. *The role of Y RNAs in DNA replication and cell growth*

4.2. *Y RNAs as modulators of Ro60 function and cellular stress*

5. The role of Y3/Y3 in the 3'-end processing of histone mRNAs**

5.1. *The depletion of Y RNAs and their impact on pre-mRNA processing*

5.2. *The evolutionary conservation of Y3's role in histone mRNA processing*

5.3. *Y3** ncRNA is essential for histone mRNA processing*

5.4. *Y3** ncRNA promotes integrity and dynamics of histone locus bodies*

Future perspective

References

Publications

Appendix

Abstract

Research progress over recent years revealed that gene expression is significantly modulated by non-coding RNAs. The main focus of this doctoral thesis was the functional characterization of a specific family of non-coding RNAs called Y RNAs. Eukaryotic Y RNAs are ~80-110 nts in length, highly conserved and transcribed by RNA polymerase III. Although already discovered in the early 1980's, little is known about the role of Y RNAs in eukaryotic cells. To identify proteins associated with Y RNAs we performed RNA pulldowns of all four human Y RNAs followed by mass spectrometry. This confirmed previously reported but also identified novel Y RNA-binding proteins including the cytoplasmic IGF2 mRNA-binding protein 1 (IGF2BP1). The analysis of the Y3-IGF2BP1 association revealed that IGF2BP1 binds the single stranded Y3-loop via its four KH-domains. Furthermore we identified the association of mRNA processing factors with Y1 and Y3. Depletion of these ncRNAs by chimeric antisense oligonucleotides (ASOs) caused a significant 3'-end processing defect of replication-dependent histone mRNAs. On the contrary, 3'-end processing of other mRNAs remained largely unaffected. Surprisingly, Y3's role in modulating the 3'-end processing of histone mRNAs is not conserved in mouse-like rodents (*muroidea*). Intriguingly, although *muroidea* express Y3 they lack a smaller Y3-variant, termed Y3**. This smaller RNA (~60 nts) was described before but not characterized in detail except reports on its expression in non-*muroidea* mammals like humans. As its precursor Y3, Y3** associates with 3'-end processing factors like the cleavage and polyadenylation specificity factor (CPSF). Whereas ASO-directed depletion results in a decrease of both, Y3 and Y3**, siRNA-directed knockdown only affects Y3. Strikingly, the 3'-end processing of histone transcripts was only perturbed by the ASO-dependent depletion of Y3 and Y3** indicating that Y3** is essential. Furthermore Y3** but not Y3 associated with histone mRNAs in RNA pulldown analyses. In agreement, the depletion of Y3/Y3** impaired the morphology of histone locus bodies (HLBs) which are the sites of histone mRNA synthesis and processing in mammalian cells. Moreover, the morphology of HLBs upon Y3/Y3** depletion was associated with compromised protein dynamics in these nuclear bodies. In conclusion, these findings indicate that Y3** ncRNA is essential for the 3'-end processing of histone mRNAs. We propose that Y3** promotes the 3'-end processing of canonical histone mRNAs by acting as a scaffolding RNA, recruiting processing factors to HLBs. To our knowledge this is the first function which could be assigned to Y3**. Moreover, our studies, in particular the analyses of Y RNA-associated proteins, sets the stage for investigating Y RNA functions in further detail.

1. Non-coding RNAs (ncRNAs)

The central dogma of molecular biology describes the transfer of genetic information by cellular molecules [1, 2]. Accordingly, deoxyribonucleic acid (DNA) can be transcribed into ribonucleic acid (RNA). RNA on the other hand can serve as the template for the translation into proteins. Thus protein encoding RNA is the essential link to transfer the genetic information from DNA to proteins and is therefore called messenger RNA (mRNA).

Besides the essential class of mRNAs, also non-coding RNAs (ncRNAs) were found in all organisms. This type of RNA is transcribed, but in contrast to mRNAs not translated into protein. Over the years it emerged, that most of the genomes are transcribed and the respective transcriptomes mainly consist of ncRNAs, especially in higher eukaryotes. Due to the larger genome and the increase of transcribed repetitive elements in eukaryotic genomes, it was proposed that most of these ncRNAs are 'junk' and therefore without any cellular function. However, more and more cellular functions are assigned to ncRNAs nowadays indicating that ncRNAs in fact serve essential roles in modulating diverse cellular processes.

NcRNAs represent a diverse ensemble of transcripts in respect to size, structure, subcellular localization and presumably cellular functions. In eukaryotes, ncRNAs are synthesized by all three RNA polymerases from individual genes (e.g. tRNAs and snRNAs) or arise by RNA-processing of pre-mRNAs (e.g. snoRNAs). They range in size from ~20 nucleotides (e.g. miRNAs, piRNAs and siRNAs) to several thousand nucleotides (e.g. MALAT1 and XIST). At the structural level longer ncRNAs can be mRNA-like, which includes typical mRNA-modifications (5'-capping, splicing and polyadenylation; e.g. H19). Shorter ncRNAs usually appear compact and are highly structured (e.g. snRNAs and snoRNAs). Many ncRNAs are poorly conserved on the nucleotide level throughout evolution, but often retain their important structural properties and functions. Accordingly, it was proposed that ncRNAs (especially long ncRNAs) undergo accelerated evolution, compared to mRNAs, caused by a lower selection pressure on individual nucleotides [3]. Due to the different characteristics of ncRNAs, the classification as well as identification of ncRNAs remain challenging and also impede the investigation of novel ncRNA functions.

2. NcRNA synthesis by RNA polymerase III

The RNA polymerase III (POLIII) is one of three multi-subunit RNA polymerase complexes found in eukaryotes. As for the other polymerases, POLIII is recruited to specific *cis*-elements on the DNA (promoters), where it starts to progressively synthesize RNAs of up to several hundred nucleotides in length. Notably, POLIII transcribed genes exclusively encode for ncRNAs, which do not associate with nuclear mRNA processing complexes. As a result, most POLIII-synthesized RNAs are neither 5'-m⁷G-capped, spliced nor 3'-polyadenylated. In fact, nascent POLIII-transcripts usually have 5'-triphosphates (pppN), which can be methylated at the γ -phosphate to increase RNA-stability (e.g. 7SK, mediated by the capping enzyme MEPCE; [4]). POLIII transcripts usually terminate at an oligo-U stretch (in vertebrates at least U₄; [5, 6]). This RNA-sequence is recognized by the nuclear RNA-binding protein La, which has a high affinity for UUU-OH containing RNAs [7]. La-binding is considered to stabilize the nascent transcripts and presumably promotes proper RNA maturation [8]. However, some POLIII-transcripts lose this terminator sequence during their lifecycle due to nucleolytic processing and accordingly also La-association (e.g. 5S, tRNAs and Y RNAs). Notably, ncRNAs synthesized by POLIII can accumulate to very high amounts in the cell. This is due to the high stability of many of those transcripts and the efficient and robust POLIII transcription machinery. Furthermore POLIII was shown to efficiently perform a termination-reinitiation process, which ensures for multiple rounds of transcription from a single activated gene [9].

POLIII-genes are historically classified according to their type of transcription initiation. Three different types of POLIII-genes have been described so far, which are each characterized by their unique *cis*-elements and gene-associated protein complexes (Figure 1).

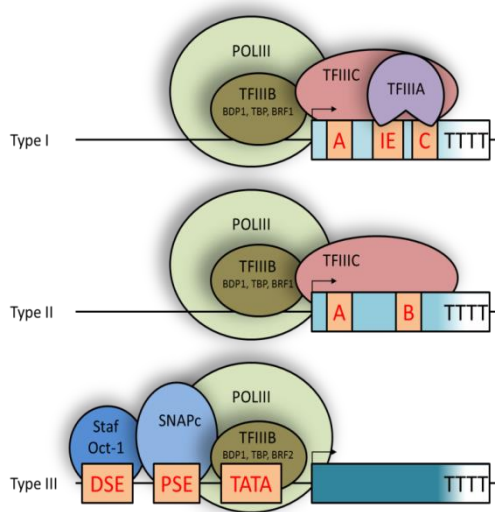


Figure 1. Types of POLIII-genes. The schematic shows the different types of eukaryotic POLIII-genes according to proteins of the respective transcription machinery. These include various transcription factors (TFIIIA, TFIIB, TFIIC, SNAPc, Staf and Oct-1). TFIIB comprises three subunits [BDP1, TBP and BRF1 (Type I and II) or BRF2 (Type III)]. The terminator signal is indicated as T₄. *Cis*-elements bound by transcription factors are colored in red (A – A-box, B – B-box, C – C-box, IE – intermediate element, TATA-box, PSE/DSE – proximal/distal sequence element). Figure adapted from [10, 11].

2.1. NcRNAs transcribed from type I and II POLIII-genes

The type I and II POLIII genes are usually referred to as internally initiated genes. Accordingly these genes contain transcription factor binding sites, which are located within the transcribed part of the gene. The multi-protein transcription factor III C (TFIIIC) associates with the A-box (Type I and II) and the B-box (Type II) to recruit transcription factor III B (TFIIIB). The TFIIIB-complex in turn can then recruit the RNA polymerase to initiate transcription. Type I genes additionally contain the intermediate element and the C-box, which are recognized by transcription factor III A (TFIIIA) to improve the recruitment of TFIIIB/POLIII (Figure 1). Although the basal transcription of type I and II genes is initiated internally, it was shown that flanking sequences can increase the transcriptional output [5].

Most of the POLIII transcribed genes are of type I or II. It was suggested that this is due to their essential role in cell growth. Three major classes of ncRNAs, all involved in protein synthesis, are encoded by type I or II POLIII genes. Type I genes encode for the 5S rRNA, a ~120nt long ncRNA which is an essential part of the large subunit of the ribosome. Many aspects of the life cycle of 5S rRNA are not known in detail, but it was proposed that 5S associates with the La protein after transcription. As for other small ncRNAs exonucleolytic 3'-end trimming occurs in the nucleus, which facilitates La dissociation and nuclear export [12]. In the cytoplasm 5S can form a ribonucleoprotein particle (RNP) with RPL5, which is then imported back into the nucleus and incorporated into the 60S subunit of the ribosome [13].

The vast majority of type II genes encode for tRNAs and 7SL RNAs. Eukaryotic tRNAs are synthesized as precursors, which are trimmed at their 5'- and 3'-ends by different endo- and exonucleases to yield 'cloverleaf'-structured tRNAs [14]. Further maturation steps including splicing, editing, CCA-addition and aminoacylation at the 3'-end are performed to produce functional aminoacylated tRNAs. These RNAs act as amino acid donors in the process of mRNA translation facilitated by the ribosome. 7SL RNA on the other hand functions as a scaffold for a cytoplasmic RNP called the signal recognition particle (SRP). The SRP recognizes specific peptide sequences (signal peptide) emerging from newly synthesized proteins at the ribosome [15]. Due to association with the signal peptide, translation is slowed down and the SRP transfers the ribosome to the endoplasmic reticulum (ER). Here it can associate with the SRP-receptor, which stimulates translocation of the growing amino acid chain into the ER-lumen. Therefore the SRP and 7SL are essential for the synthesis of ER-associated and secreted proteins.

2.2. NcRNAs transcribed from type III POLIII-genes

Type III genes are usually referred to as externally initiated POLIII-genes and more closely resemble the transcription initiation of other RNA polymerases such as POLII. The essential transcription factor SNAPc binds to the proximal sequence element (PSE) in type III genes to recruit TFIIB, which binds to the TATA-box in close proximity to the transcription start site. These factors can recruit RNA polymerase III to start RNA synthesis. Among other transcription factors Staf and Oct-1 were shown to enhance the transcription rate of type III genes due to association with the distal sequence element (DSE; Figure 1).

The first experiments to investigate the structure of type III genes were conducted with genes encoding for the U6 snRNA. This nuclear ncRNA is exclusively found in eukaryotes and is part of the spliceosome responsible for intron removal in the process of splicing. Like all other spliceosomal RNAs, U6 forms a RNA-protein complex, the U6 snRNP. U6 can partially hybridize with U4 snRNA, which constitutes the U4/U6 di-snRNP [16]. Furthermore U5 snRNA can join this complex to form the spliceosomally active U4/U6.U5 tri-snRNP [17]. The tri-snRNP joins the A-complex of the spliceosome (mainly consisting of U1/U2 snRNPs) to constitute the B-complex. Within this process U4 leaves the complex and U6 hybridizes with U2 to form the 'heart' of the spliceosome together with the protein Prp8 [18].

Another essential type III gene encodes for the 7SK ncRNA. This nuclear ncRNA associates with the positive transcription elongation factor (P-TEFb), consisting of CDK9 and cyclins [19]. The P-TEFb complex can phosphorylate multiple nuclear substrates including the C-terminal domain of RNA polymerase II. These modifications activate POLII and ensure productive transcription elongation. 7SK binding inactivates P-TEFb and inhibits its positive effect on POLII mediated transcription [19]. It was proposed that the sequestering of P-TEFb by the 7SK RNP is a major regulatory step in POLII driven transcription [20].

Taken together there is substantial evidence that ncRNAs synthesized by POLIII perform or modulate essential roles in a variety of cellular processes. Many of these ncRNAs are highly conserved and perform similar functions from protozoa to mammals. Y RNAs represent a particular family of POLIII synthesized ncRNAs (type III), which were the main focus of this thesis.

3. The non-coding Y RNAs

Y RNAs constitute a family of highly conserved ncRNAs synthesized by POLIII. They usually range in size from approximately 80 to 110nts (Figure 2). They were discovered over 30 years ago based on their ability to be co-precipitated with anti-Ro60 and/or anti-La auto-antibodies [21]. As many other POLIII transcripts, Y RNAs comprise a 5'-triphosphate and a 3'-oligo-U-tail [22, 23]. The stem-loop structure of Y RNAs is highly conserved throughout evolution (Figure 2). The 5'- and 3'-ends of Y RNAs form the conserved stem (each ~20nts) and are connected by a flexible loop region (40-70nts). Notably, the Y RNA stem contains unpaired nucleotides (bulges), which contribute to protein association, in particular the binding of Ro60 [24].

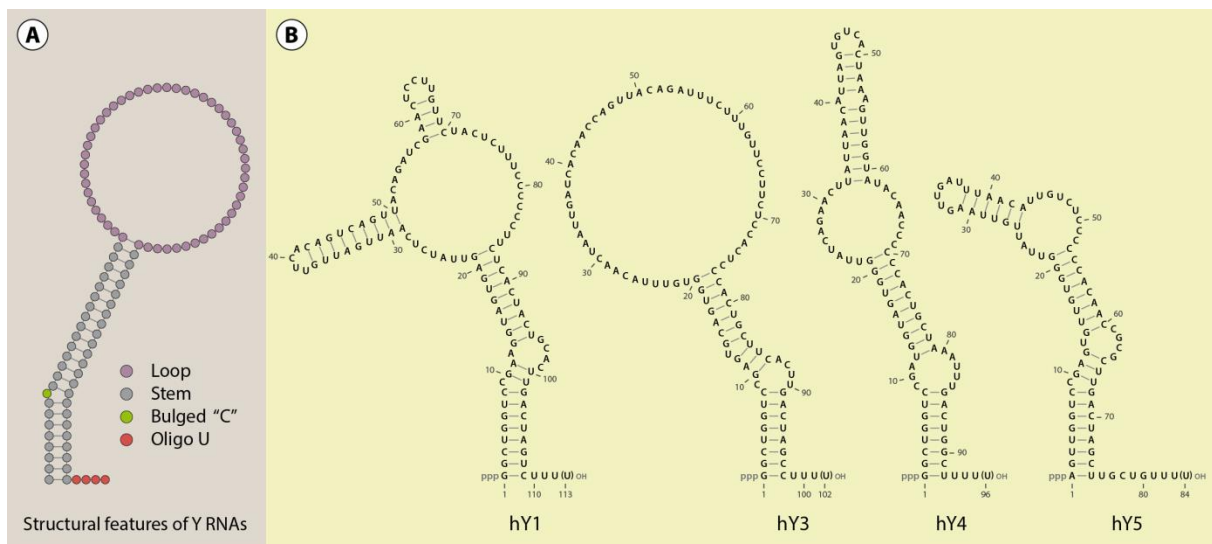


Figure 2. Y RNA structure. (A) The characteristic features of Y RNAs are depicted in a schematic structure model. (B) The sequences and selected experimentally determined secondary structures of the human Y RNAs are shown (taken from [25]). Note that Y RNA structures are considered to be quite flexible especially within the loop-region as confirmed in structure probing experiments [26, 27].

3.1. Evolution of Y RNAs

Y RNAs homologs were identified in a variety of species ranging from bacteria to vertebrates. Interestingly the existence of experimentally verified Y RNAs always coincides with the presence of the RNA-binding protein Ro60 (summarized in Table 1). This is presumably due to the highly conserved interaction of Ro60 with the bulged stem of Y RNAs [24]. The binding of Ro60 to Y RNAs was shown to increase the stability and stabilize the structural fold of these ncRNAs. It is therefore assumed that Ro60 and Y RNAs co-evolved [25, 28].

Table 1. Ro60 and Y RNA homologs identified in the three domains of life. For some species Ro60 or Y RNA homologs can just be predicted from sequenced genomes (genetic evidence) and still have to be validated experimentally.

Domain	Ro60 homolog identified	Y RNA homolog identified
Bacteria	Diverse for example: <i>Deinococcus radiodurans</i> <i>Salmonella typhimurium</i>	Diverse for example: <i>Deinococcus radiodurans</i> <i>Salmonella typhimurium</i>
Archaea	<i>Haloarcula amylolytica</i> (gen. evidence)	Not investigated
Eukarya	Chlorophyta: <i>Volvox carteri</i> (gen. evidence) <i>Chlamydomonas reinhardtii</i> (gen. evidence)	Not investigated
	Plants: presumably not present	Not investigated
	Fungi: presumably not present	Not investigated
	Nematoda: <i>Caenorhabditis elegans</i> <i>Caenorhabditis briggsae</i>	<i>Caenorhabditis elegans</i> <i>Caenorhabditis briggsae</i> (prediction)
	Insects: <i>Drosophila melanogaster</i> (gen. evidence) <i>Apis mellifera</i> (gen. evidence) <i>Anopheles gambiae</i> (gen. evidence)	<i>Anopheles gambiae</i> (prediction)
	Vertebrates: Diverse for example: <i>Homo sapiens</i> <i>Mus musculus</i> <i>Xenopus laevis</i> <i>Danio rerio</i>	Diverse for example: <i>Homo sapiens</i> <i>Mus musculus</i> <i>Xenopus laevis</i> <i>Danio rerio</i>

Presumably due to the essential role of Ro60-binding, Y RNAs show the highest degree of conservation within their stem region (Figure 3). Among the different Y RNA paralogues, Y3 seems to be the most conserved Y RNA at least in the vertebrate lineage [29]. Accordingly it was proposed that other Y RNAs arose by gene duplication from an ancestral Y1/Y3-like ncRNA [30]. Future studies will have to reveal, if every species expressing a Ro60 protein also possesses a Y RNA homolog. Due to limitations in the number of sequenced genomes and the short length of Y RNAs it remains difficult

to identify Y RNA homologs at least in non-vertebrata. However, Y RNA sequences can be used to recapitulate the evolution in the vertebrate lineage [31].

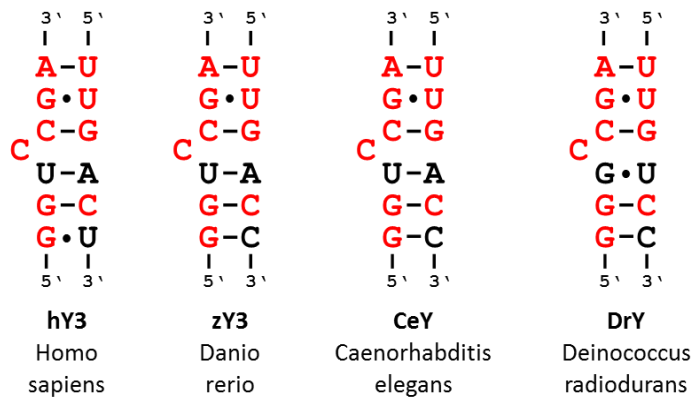


Figure 3. Y RNA conservation. The Ro60-binding sites in the stem region of Y RNAs from different species are depicted. For better comparison the secondary structure arrangement obtained by crystallographic studies of a Y RNA-fragment was chosen [32]. Note that many nucleotides show perfect conservation (red).

3.2. Y RNA genes and expression patterns

All identified eukaryotic Y RNAs are synthesized by POLIII. More precisely they resemble type III genes, which contain PSE and TATA *cis*-elements (see also Figure 1). Unlike many other POLIII-genes Y RNA genes appear as single copies in the respective genomes, which are organized as a genomic cluster in vertebrates (Figure 4). It was recently shown that various pseudogenes derived from Y RNAs exist in vertebrate genomes [31, 33]. Many of these pseudogenes lack the characteristic type III-gene features and are mutated at critical nucleotides (e.g. C9). Therefore one can assume that most of these pseudogenes do not contribute significantly to Y RNA expression or functions of this ncRNA family. It was also proposed that Y RNA pseudogenes originated by retro-transposition [33].

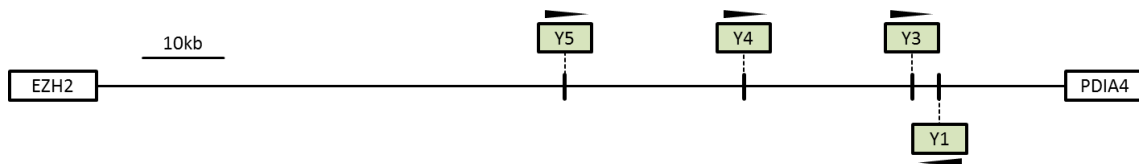


Figure 4. The human Y RNA cluster. The location of the human Y RNA genes on chromosome 7q36 is indicated. Y RNA genes are flanked by the protein coding genes EZH2 (enhancer of zeste 2 polycomb repressive complex 2 subunit) and PDIA4 (protein disulfide isomerase family A, member 4). The polarity of the Y RNA genes is indicated by an arrowhead.

The number of Y RNA genes in different species can vary substantially. In the vertebrate lineage bony fish seem to have just one gene for an Y3-like ncRNA. In most other vertebrate species four Y RNA genes expressing Y1, Y3, Y4 and Y5 orthologs have been identified. Interestingly some species seem to have lost specific Y RNA genes. Mouse-like rodents (*muroides*) for example retained just Y1- and Y3-encoding genes, but apparently acquired other rodent specific ncRNA genes (e.g. 4.5S RNA genes). It was proposed, based solely on gene predictions *in silico*, that in nematodes multiple

copies of different Y RNA genes may exist (>10). However, this needs further experimental validation [34].

Bacterial Y RNA genes are usually located near the respective Ro60-homolog in an operon-like fashion (shown for e.g. *D. radiodurans*; [35]). It is assumed, that due to the spacial proximity of the Ro60 and Y RNA genes, these can be induced simultaneously under certain environmental conditions, e.g. UV-irradiation [35]. Notably just a few percent of the sequenced bacterial genomes contain Ro60 and Y RNA homologs. Future studies will have to reveal, why the Ro60-Y RNA complex is important for only some bacteria. Additionally, so far it was not determined if Ro60 and Y RNAs were formerly present in all bacteria or acquired at a later time point.

Y RNA levels can substantially vary between tissues and cell types, although they seem to be expressed ubiquitously. We investigated Y RNA expression in a set of distinct mouse tissues by infrared Northern blotting (Figure 5). This demonstrated that murine Y RNAs are highly expressed in brain, lung heart, stomach, kidney, ovary, adipose tissue and skeletal muscle. Future studies will have to reveal cell type specific expression of Y RNAs and their roles in the respective cells and/or tissues. Notably, we established a knockdown procedure to analyze Y RNA functions *in vivo* (Figure 6). To this end, chimeric antisense oligonucleotides (ASOs) were intraperitoneally injected into mice. After four days the mice were sacrificed and Y RNA depletion was monitored in different tissues by Northern blotting. These experiments showed that endogenous Y3 RNA can be significantly reduced by ASO-injection in mouse tissues like the liver (Figure 6). Once murine Y RNA functions have been identified, this procedure will be useful to validate such functions also *in vivo*.

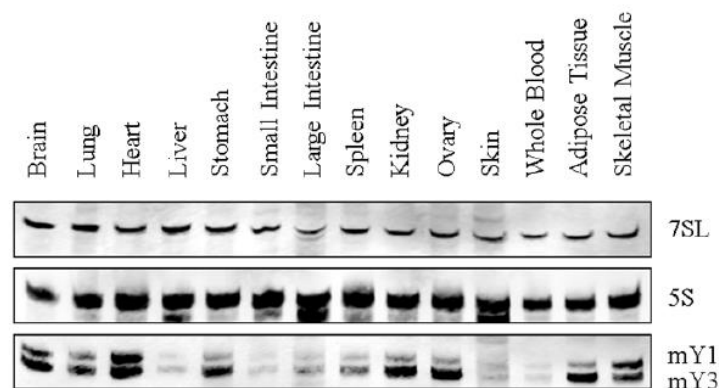


Figure 5. Murine Y RNA expression. Total RNA was isolated from nude mice and subjected to Northern blotting to analyze Y RNA levels (2,5 µg/lane). 7SL and 5S RNAs served as loading controls. (taken from [25])

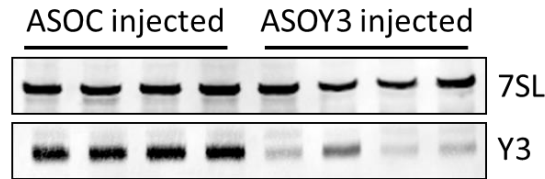


Figure 6. Y RNA depletion in mice. Eight C57BL/6 mice were injected with ASOs (either control or targeting Y3 RNA) intraperitoneally. After four days the mice were sacrificed, total RNA was isolated from the liver and subjected to Northern blot analyses (5 µg/ lane). These blots were incubated with probes hybridizing to Y3 and 7SL (loading control). Note that up to 75% of liver Y3 RNA can be depleted with this method (unpublished data).

3.3. Processing of Y RNAs

Since the discovery of Y RNAs the existence of smaller Y RNA fragments had been observed [23]. The majority of Y RNA variants seem to be shortened at their 3'-end. These processing events obviously occur at the 3'-end of Y1, Y3 and Y4 RNAs and usually result in Y RNAs shortened by 4-5 nucleotides (Figure 7). So far, no 3'-shortened variant of Y5 was observed. Formerly these trimmed variants were named differently, such as 'Y2' for the Y1 variant and 'Y3*' for the Y3 variant. The 3'-end trimming of POLIII transcripts is a common phenomenon, also described for other RNAs such as 5S rRNA [36]. The impact of 3'-end processing on Y RNA function is barely understood. It is assumed that the association of POLIII transcripts with the La protein at the oligo-U tail inhibits nuclear export. Therefore removal of this tail would lead to enhanced nuclear export. Indeed it was shown, that the La protein can inhibit the nuclear export of Y1 [37]. Furthermore upon Ro60 depletion Y RNA levels drop drastically, but the remaining Y RNAs have elongated 3'-ends and accumulate in the nucleus [38]. This argues for a positive role of Ro60 and a negative role of La in the nuclear export of Y RNAs. Consistently, the more nuclear Y5 RNA retains its original oligo-U tail (Figure 7; [39]). Notably another variant of Y3, termed 'Y3**', was described previously [23]. This severely 3'-shortened variant (total length of ~60nts) terminates within the loop of Y3 RNA. The processing mechanism as well as the role of this ncRNA has not been determined so far.

	Y1	Y3	Y4	Y5
Full length	...ACUAG UCUUU	...ACUAG CCUUU	...ACUGG CUUU	...UGCUGUUU
Processed	...ACUAG-----	...ACUAG-----	...ACUGG----	...UGCUGUUU

Figure 7. The 3'-end processing of human Y RNAs. The sequences of the human full length and processed Y RNA 3'-ends are shown. Removed nucleotides of the respective Y RNAs are colored in red (unpublished results obtained by 3'-RACE from human HEK293 RNA).

Notably also Y RNA derived fragments (20-30 nucleotides) have been identified in a variety of tissue samples and cell lines [40-42]. These fragments mostly originated from the stem regions of all four Y RNAs. It has been shown, that these fragments exist in a variety of cells under normal growth conditions, but their levels sharply increase upon stress conditions like apoptotic stimuli or poly (I:C) treatment [40, 43]. The biogenesis of Y RNA fragments is independent of the Dicer protein and they are not associated with Argonaute proteins. Thus it appears unlikely that these fragments are acting in a miRNA-like fashion [43]. Accordingly, antisense reporter analyses could not confirm any influence on the translation of reporter mRNAs [42]. Y RNAs are degraded under apoptotic conditions, which lead to the accumulation of Y RNA-stem derived fragments. Therefore it was proposed that Ro60 protects the Y RNA stem fragments from being further degraded [40]. Interestingly Y RNA-derived fragments were found in the blood and their level may change with age [44, 45]. Whether this is of any clinical significance remains to be elucidated.

The Y3** ncRNA was of particular interest for this thesis. Our studies provided strong evidence that this ncRNA is essential for histone mRNA 3'-end processing. This was supported by the ASO-directed depletion of Y3 and Y3**, which led to an increase of misprocessed histone mRNAs in HEK293 cells (see Köhn et al. 2015 Figure 3). To analyze Y3** in more detail we determined the exact sequence of Y3**, since only the 5'-end of Y3** was properly characterized. Accordingly, we performed 3'-RACE analyses on total human RNA isolated from HEK293 cells. This demonstrated that in eight out of ten sequenced clones Y3** was terminated at U60 or U61 of the Y3 sequence (Figure 2). To verify these findings, the human Y3 gene under the control of the endogenous Y3 promoter was overexpressed in HEK293 cells, which led to increased levels of Y3 as well as Y3**. Furthermore T60A and T61A mutations were introduced into the Y3 gene (Figure 8). Interestingly the T61A mutated gene still led to the synthesis of Y3 and Y3**. The T60A mutated gene on the other hand just allowed overexpression of Y3, exogenous Y3** was not detectable any more in Northern blot analyses (Figure 8). Therefore we assume, that U60 is critical for the production of Y3** and thus consider it unlikely that Y3** results from premature termination of POLIII-driven transcription. In support of this notion Y3**-synthesis was unaffected by the T61A mutation. Instead of premature termination, we propose that Y3** is produced by nucleolytic cleavage of Y3, a process which might be facilitated by an endonuclease requiring U60. Future experiments will have to validate this hypothesis, for instance by the depletion of endonucleases (RNAi) and subsequent Northern blot analyses to investigate Y3** levels.

Subcellular fractionation of human HEK293 cells revealed, that Y3** is present in both, nuclear and cytoplasmic compartments (Figure 9). Y3** is not detectable in RNA isolated from cells, which originated from mouse-like rodents (*muroidea*, also see Figure 18 and Köhn et al. 2015 Figure 3).

Preliminary evidence suggests, that this is due to nucleotide variations in the 5'-part of the Y3 sequence, which may decrease the stability of Y3** drastically, while maintaining Y3 ncRNA in *muroidea* (see Köhn et al. 2015 Figure 4 and S3). However, also in human cells Y3** does not accumulate to high levels (e.g. ~6% of Y3 in HEK293 cells), suggesting that: a) the processing of Y3 into Y3** is rather slow, b) Y3** is produced from a minor portion of Y3 or c) the stability of Y3** is comparatively low (Figure 8). If Y3** serves additional roles, besides the 3'-end processing of histone mRNAs (see chapter 5), remains largely elusive. Proteomic approaches (data not shown), suggest that Y3** may have a role connected to nuclear RNPs, since many nuclear proteins (e.g. spliceosomal proteins) associate with Y3** but not with Y3. These studies also showed that Y3 and Y3** have overlapping, but not identical interaction patterns.

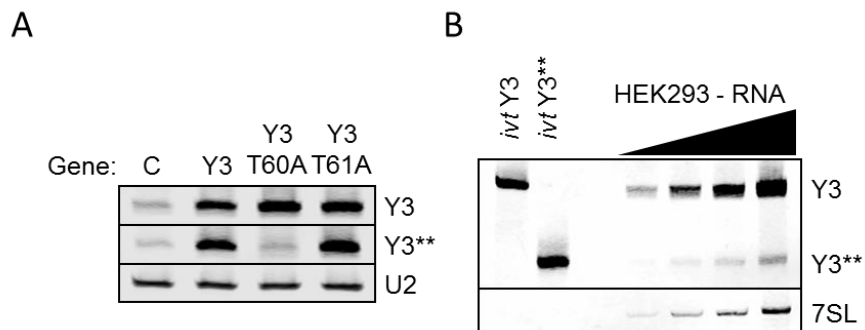


Figure 8. Expression of Y3.** (A) HEK293 cells were transfected with plasmids containing wild type (Y3) or mutated (T60A, T61A) human Y3 genes. Transfections with empty vector served as a control (C). After 48h the cells were harvested, total RNA was isolated and subjected to Northern blot analyses with specific probes for Y3/Y3** as well as the loading control U2. (B) Increasing amounts of HEK293 total RNA were loaded on TBE-urea gels and subjected to Northern blotting. Y3 and Y3** RNAs were detected with the same Northern probe and *in vitro* transcribed RNAs (*invt* Y3, *invt* Y3**) served as references. 7SL RNA served as loading control (taken from Köhn et al. 2015 Figure 4 and S3).

3.4. Subcellular localization of Y RNAs

The localization of Y RNAs has been studied in a variety of species by diverse methods. The vast majority of these studies agree that Y RNAs primarily localize to the cytoplasm, where they exist in complexes with Ro60 and presumably other RNA-binding proteins. Upon injection into *Xenopus* oocytes Y RNAs (mostly shown for Y1) are rapidly and completely exported to the cytoplasm, a process which is inhibited by the La protein [37]. In contrast, Y5 differs in this respect from the other Y RNAs, since a significant amount of this RNA is retained in the nucleus (Figure 9; [39]). Accordingly one can speculate that the susceptibility for 3'-trimming (Y1, Y3 and Y4) correlates with the subcellular localization of Y RNAs (see chapter 3.3.). In respect thereof the export adapter for Y RNAs

would be inhibited by Y RNA 3'-ends and La-association. Previous studies suggested that Exportin 5 (XPO5) is a promising candidate exporter for Y RNAs, since it binds short stem-loop RNAs (such as pre-miRNAs) and also associates with Y1 *in vitro* [46].

According to fluorescence *in situ* hybridization (FISH) analyses Y RNAs are not enriched at specific sites in the cytoplasm but show a rather ubiquitous, granular distribution in the cytoplasm. These observed cytoplasmic granules might indicate Y RNA containing Ro60-RNPs [47]. Notably, Y RNAs also localize to the perinucleolar compartment (PNC; [48]), a nuclear body tightly associated with the nucleolus. The exact role of PNCs, which are enriched for splicing modulators like PTBP1 and RAVR1 proteins, is only poorly understood so far. However, the localization to PNCs is not Y RNA specific, since other POLIII transcripts are also enriched in PNCs [48]. This led to the hypothesis that newly synthesized POLIII transcripts might be stored and transported from PNCs [49]. Furthermore, the PNC marker protein PTBP1 was shown to directly bind to Y1 and Y3 RNAs, an interaction which might occur in PNCs [50].

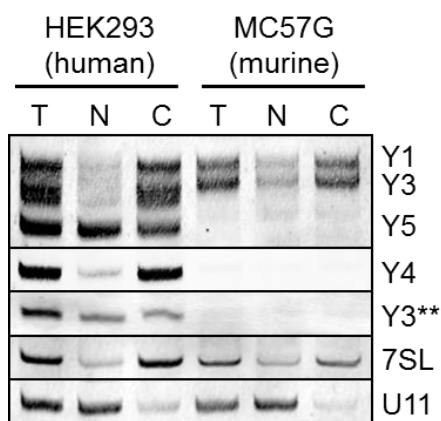


Figure 9. Subcellular localization of Y RNAs. Nuclear (N), cytoplasmic (C) and total (T) RNA from human HEK293 and murine MC57G cells was analyzed for Y RNAs by Northern blot analyses. 7SL and U11 served as cytoplasmic and nuclear marker RNAs, respectively (taken from Köhn et al. 2015 Figure 4).

3.5. Y RNA-associated proteins

A variety of Y RNA-associated proteins could be identified so far (reviewed in [25]). Amongst those are proteins which associate with all Y RNA species (core proteins, e.g. La and Ro60) and those which bind just some Y RNAs (accessory proteins, e.g. IGF2BPs and PTBP1). Presumably the Y RNA core proteins are mostly responsible for Y RNA biogenesis and stability, whereas accessory proteins may confer more specific functions to individual Y RNAs.

To get a more systematic view on Y RNA-associated proteins we performed RNA pulldowns in HEK293 cell lysates. Therefore we labeled all four human Y RNAs with biotinylated UTP during *in vitro* transcription. These randomly biotinylated Y RNAs were then immobilized on a paramagnetic streptavidin-resin and incubated with cell lysate derived from human HEK293 cells. The eluted proteins were resolved on a SDS-polyacrylamide gel and subjected to mass spectrometric (MS)

analyses (Figure 10). Strikingly, protein class determination revealed ‘nucleic acid binding’ to be the most prominent protein class in Y RNA pulldowns (Figure 10).

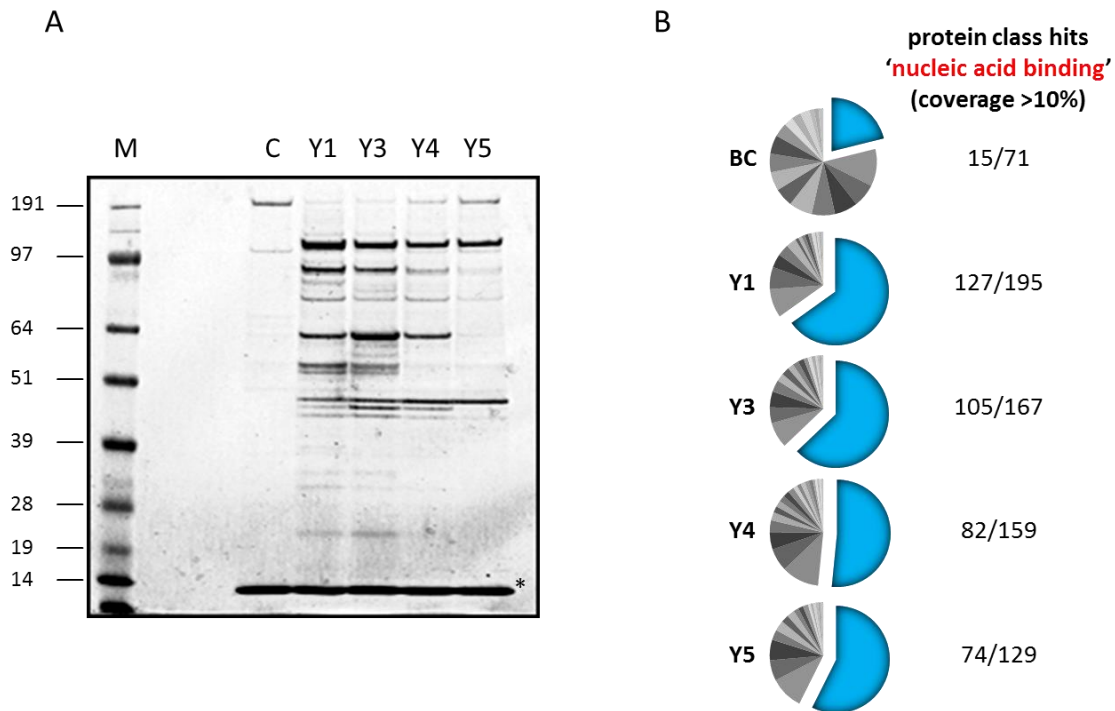


Figure 10. Identification of Y RNA-associated proteins. (A) Eluted proteins from Y RNA pulldowns (Y1, Y3, Y4 and Y5) were subjected to SDS-PAGE together with a protein marker (M, sizes in kDa) and stained by Coomassie Brilliant Blue. Beads only (C) served as background control. The asterisk indicates the streptavidin protein. (B) After protein identification by MS analyses, database research was performed with PANTHER protein class determination (taken from Köhn et al. 2015 Figure 1 and S1; [51, 52]).

With the exception of APOBEC3G, we could confirm all previously reported Y RNA-binding proteins by the established procedure (reviewed in [25]). These included Y RNA core proteins (La and Ro60) as well as accessory proteins (NCL, PTBP1, HNRNPK, IGF2BP1 and PUF60). Furthermore this method allowed us to explore new functions for Y RNAs based on their associated proteins, e.g. the role of Y3/Y3** in the processing of replication-dependent histone mRNAs (see also chapter 5).

3.6. The Y RNA core proteins – La and Ro60

The first proteins shown to associate with Y RNAs were La and Ro60 [21]. The immunological disorders ‘Systemic lupus erythematosus’ (SLE) and ‘Sjögren's syndrome’ (SS) are characterized by the production of a variety of autoimmune-antibodies targeting healthy cells, which finally can cause apoptosis and inflammation in a variety of tissues [53]. Anti-La and anti-Ro60 were among the antibody species detected in SLE/SS patients and belong to the group of anti-nuclear antibodies (ANA). The reason why antibodies against these two RNA-binding proteins (RBPs) are produced in the

patients remains largely unknown. However in times where antibodies for immunological experiments (immunoprecipitation, Western blot) were rare, these auto-antibodies allowed the investigation of the targeted proteins as well as the associated diseases itself. Today the testing for ANAs is one major diagnostic step for the identification of immunological diseases like SLE or SS.

Initial immunoprecipitation studies with sera of anti-La/Ro60 positive SLE/SS patients showed that these proteins associate with cellular RNAs. Amongst those were RNA species of about 80-110nts in length, which were named cytoplasmic Y RNAs in analogy to the nuclear U RNAs [21]. Formerly five different Y RNA species were detected in human (Y1, Y2, Y3, Y4 and Y5) and three Y RNAs in mouse cells (Y1, Y2 and Y3). Later Y2 was omitted since it was discovered that this RNA is a processed variant of Y1 (also see chapter 3.3.).

The eukaryotic La protein is a mainly nuclear RBP of about 46 kDa in human (Gene symbol: SSB). It is a multi-domain protein, which has a high affinity for RNAs with UUU-OH at their 3'-end (reviewed in [54]). The RNA-binding of La is mainly facilitated by its N-terminal domain (NTD) consisting of a so called 'La-motif' as well as a RNA recognition motif (RRM). Since La binds nascent POLIII transcripts it was suggested, that it has a general role in the maintenance of those transcripts. In respect to Y RNAs the function of this protein is not well understood except its inhibitory role in the nuclear export of nascent Y RNAs (see also chapter 3.3. and 3.4.). By chromatin immunoprecipitation (ChIP) it was shown that La is present at the genomic loci of Y RNA genes. However, which functions it may serve there remains elusive [55]. We and others found La to be associated with all four human Y RNAs in RNA pulldown experiments (see chapter 3.5.). Furthermore, endogenous Y RNAs as well as Y3** could also be co-immunoprecipitated with Flag-tagged human La protein (data not shown). Notably, Y RNAs associating with La were slightly longer than the bulk of cellular Y RNAs, supporting the notion that La associates with nascent RNAs still containing the oligo-U tail. The depletion of cellular La protein by RNAi did not show any alteration of global Y RNA levels (data not shown). Future studies will have to reveal, which aspects besides the nuclear export of the Y RNAs may be conducted by the La protein. An involvement of La in the nuclear surveillance of Y RNAs including folding or modification appears likely but solid evidence is still lacking.

The Ro60 protein is a ring shaped RBP of approximately 60 kDa in size (Gene symbol: TROVE2). The crystal structure of Ro60 revealed that most of the protein ring is formed by a helical HEAT-repeat domain, which is closed by a vWFA-domain [32]. The HEAT-repeat ring also comprises the majority of the two distinct RNA-binding surfaces of Ro60. The first one is located within the central cavity of the ring. RNA-binding by this cavity is mainly mediated by basic amino acid side chains protruding from different helices of the HEAT-repeats. Structural and binding studies suggested that double stranded RNA (dsRNA) with a protruding single stranded 3'-end is preferentially bound in this

cavity [32]. To date just one cellular target RNA for the Ro60-cavity was characterized in detail, which is a misfolded form of the 5S rRNA [32]. The second RNA-binding surface of Ro60 is sculptured by the HEAT-repeats at the outer side of the Ro60-ring. In accordance with the cavity, RNA-binding by the outer surface is mainly mediated by basic amino acids, which contact the phosphate backbone of the RNA. Therefore it is not surprising that RNA-binding is not tightly determined by the primary nucleotide sequence but highly structure dependent [32, 56]. Notably, this RNA-binding surface is highly conserved in all Ro60 proteins identified so far. The primary target RNAs for the outer surface of Ro60 are Y RNAs. It is likely that due to the structural constraints Y RNAs show the highest conservation at the Ro60 binding site (see also Figure 3). Importantly, the bulged C-nucleotide (usually C9) is critical for the RNA-association of Ro60. In agreement, deletions or mutations at this site strongly reduce the Y RNA-binding of Ro60 (Figure 11 and [56]). One validated role of the Ro60-Y RNA interaction is the stabilization of Y RNAs. In support of this Y RNA levels are usually drastically decreased upon depletion of Ro60. This was also confirmed by the knockout of Ro60 in mice, leading to an almost complete loss of Y RNAs (Figure 11 and [57]). Besides its role in enhancing the nuclear export of Y RNAs (see also chapter 3.4.) other functions of the Ro60-Y RNA complex have been suggested. It was proposed that Ro60 cannot bind simultaneously to misfolded RNAs and Y RNAs [32]. Therefore one could assume that Y RNA-binding might influence the capacity of Ro60 to function in RNA quality control pathways. Future studies will have to reveal other modes of Ro60-Y RNA regulation, especially when more functions can be assigned to either Ro60 or Y RNAs.

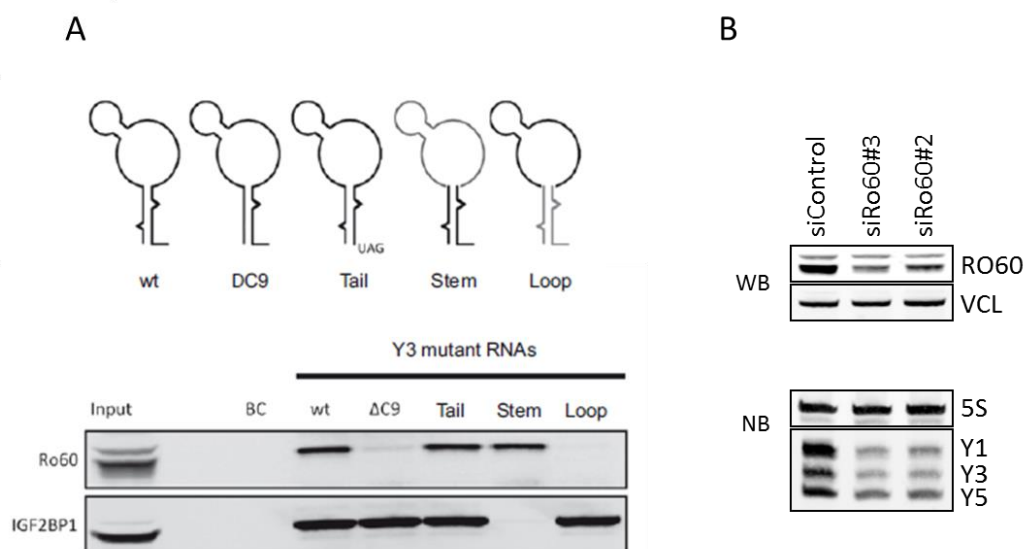


Figure 11. Y RNA-binding by Ro60. (A) Different mutants of human Y3 RNA were tested for the association of Ro60 and IGF2BP1 in RNA pull-downs (HEK293 lysate) followed by Western blotting. Ro60 binds Y3 within the RNA-stem in a C9-dependant manner. In contrast, IGF2BP1 binds the Y3-loop (taken from [58]). (B) RNAi experiments were performed to decrease the amount of Ro60 in

HEK293 cells. Western blot analyses (WB) confirmed successful knockdown of Ro60 by two distinct siRNAs. Vinculin (VCL) served as loading control. In addition, total RNA was isolated and analyzed by Northern blot analyses (NB). This revealed a decrease of Y RNA levels in Ro60 knockdown cells as assessed by probing for Y1, Y3 and Y5 RNAs. 5S rRNA served as a loading control (unpublished data).

3.7. A paradigm of accessory Y RNA-binding proteins – IGF2BPs

Accessory Y RNA-binding proteins usually associate with the distinct loops of target Y RNAs. For example, this was shown for PTBP1 and NCL which mainly bind the Y1- and Y3-loops [50, 59]. In our lab the binding of PUF60 to the Y5 RNA is currently under investigation. Preliminary results suggest that PUF60 associates with a U-rich region within the Y5-loop (unpublished). These examples provide further evidence for a plethora of accessory loop-associated Y RNA-binding proteins, a hypothesis strengthened by our Y RNA pulldown analyses (see also chapter 3.5.). The first group of novel proteins which we identified to associate with Y RNAs was the IGF2BP protein family [60].

The insulin-like growth factor II mRNA-binding proteins (IGF2BPs) constitute a family of RBPs of approximately 60 kDa in size. Three IGF2BP paralogues are expressed in mammals sharing the same domain structure (IGF2BP1, IGF2BP2 and IGF2BP3). They contain two N-terminal RRM-domains and four C-terminal hnRNP-K-homology (KH) domains. RNA-binding is readily facilitated by the four KH-domains (with major contribution of KH-3). The RRM-domains seem to be inactive in RNA-binding and may fulfill other functions such as protein-protein interactions [58, 61]. The expression of IGF2BPs is tightly controlled throughout development. All IGF2BPs are highly expressed during mouse embryogenesis, but soon after birth the levels of IGF2BP1 and IGF2BP3 decrease dramatically to barely detectable levels in most tissues [61]. IGF2BP2 on the other hand seems to be expressed also in adults. Interestingly IGF2BP1/3 are frequently re-expressed or severely upregulated in neoplasia. Accordingly, IGF2BPs are considered to be 'oncofetal' proteins. In contrast to many other RBPs, IGF2BPs are almost exclusively observed in the cytoplasm and were reported to mainly associate with mRNAs. IGF2BPs were shown to associate with the 5'-UTR, the coding sequence (CDS) or the 3'-UTR of their target mRNAs (reviewed in [61]). This was initially described when analyzing the chicken β -actin (ACTB) mRNA [62]. This mRNA was known to be localized to the leading edges of fibroblasts and migrating mesenchymal cells, where local protein synthesis might enforce high actin protein concentrations to sustain cytoskeletal reorganization and migration [63]. This working model was also strengthened by analyses in neurons, where mRNAs like ACTB have to be transported over large distances [64]. In depth analyses further revealed that an element in the 3'-UTR of the ACTB mRNA is necessary for this subcellular transport, called the 'zipcode' [65]. Soon the zipcode binding protein 1 (ZBP1), now referred to as IGF2BP1, was identified to bind this element and control ACTB mRNA localization [62]. Furthermore the binding and release of ACTB mRNA is spatially controlled by

the phosphorylation of IGF2BP1 by the Src kinase, providing an example for a phosphorylation-dependent switch of protein function [66]. Meanwhile many other target RNAs have been identified for IGF2BPs, which also includes long mRNA-like ncRNAs such as H19 or more recently HULC [67, 68]. The preferred functions of IGF2BPs seem to be the stabilization of their target mRNAs, but translation effects either due to the inhibition of translation initiation or competition with miRNA-binding were suggested as well (reviewed in [61]).

In immunoprecipitation analyses IGF2BP1 was reported to associate with Ro60 [69]. This finding prompted us to investigate, if the IGF2BP1-Ro60 interaction might involve Y RNAs. Therefore we performed immunoprecipitation as well as *in vitro* binding experiments with IGF2BP1 (ZBP1) and Y RNAs. These analyses clearly indicated that Y3 and to a lesser extent Y1 are directly bound by IGF2BP1 [60]. Furthermore we could show that all four KH-domains of IGF2BP1 are involved in Y3-binding [58]. The direct involvement of all KH-domains of IGF2BP1 was a novel and surprising finding, but it turned out that this is not exclusively observed for Y3-binding, but is also true for mRNA targets like ACTB or MYC [58]. Additionally, IGF2BP1 associates with Y3 within the loop region (~60nts, Figure 11), but all attempts to further narrow down the RNA target sequence failed since either 5'- or 3'-deletions resulted in a severely reduced association (data not shown). Similar to IGF2BP1, we observed that also the other IGF2BP paralogues (IGF2BP2 and IGF2BP3) associate with Y3, presumably by binding to the loop region. Furthermore, preliminary results suggest that IGF2BP2 also associates preferably with Y3 in a KH-domain dependent manner. Finally, the binding of Y3 to IGF2BPs was confirmed by another study which suggested that Y3 might be involved in the nuclear export not just of Ro60, but also of IGF2BP1 [70]. IGF2BP1 and Y3 are mainly cytoplasmic at steady state and do not show strong nucleo-cytoplasmic shuttling. Therefore we consider it likely that the complex exhibits a cytoplasmic role, for instance stabilization of the IGF2BP proteins and regulation of IGF2BP functions with Y3 acting as a cellular IGF2BP-competitor or chaperone. In summary we for the first time identified a small ncRNA to associate with IGF2BPs. Since the high affinity binding site for IGF2BPs within Y3 is sharply defined, future studies could use this knowledge to perform structural studies with the IGF2BP-Y3 complex. These analyses could help to understand the mode of RNA-binding by the 'oncofetal' IGF2BPs. Despite solid evidence for direct RNA-binding, the cellular role of the Y3-IGF2BP complex remains largely elusive.

3.8. The characterization of Y RNPs

The association of Y RNAs with different RBPs raised the question, if an assembly of larger Y RNA-RBP complexes (Y RNPs) occurs within the cell. It has been reported that Ro60-associated Y RNA complexes range in size from 150-550 kDa as analyzed by ion-exchange chromatography and gel filtration [71]. We could reconstitute a complex consisting of IGF2BP1, Y3 and La *in vitro* as demonstrated by electrophoretic mobility shift assay (EMSA; [60]). These experiments for the first time showed that stem- and loop-binding RBPs can associate concomitantly on one Y RNA. Future studies could analyze the fraction of Y RNAs covered by proteins in the cell and the implication of these complexes for Y RNA/RBP function. We recently started to monitor Y RNPs in glycerol gradient assays, which were originally developed for the analysis of small RNAs and associated proteins (Figure 12). These experiments revealed that the majority of extractable cellular Y RNAs exist in relatively small complexes (fractions 3-5, sedimenting at ~7-10S) similar to some other small RNAs (see 'Total RNA'). Furthermore Y RNPs do not co-sediment with ribosomes (fraction 'P') indicating that Y RNAs may not directly be involved in mRNA translation. However, co-localization of Y RNA-binding proteins and Y RNAs (e.g. PUF60 and Ro60) in glycerol gradients supports the presence of these proteins in distinct Y RNPs. In depth analyses of Y RNPs, e.g. with high resolution glycerol gradients will identify the composition of Y RNPs and thus will provide new insights for the functional roles of these protein-RNA complexes. A detailed study with the aim to analyze one particular Y5 RNP is currently under investigation in the lab. Preliminary results suggest that Y5 can concomitantly associate with the RBPs La, Ro60 and PUF60.

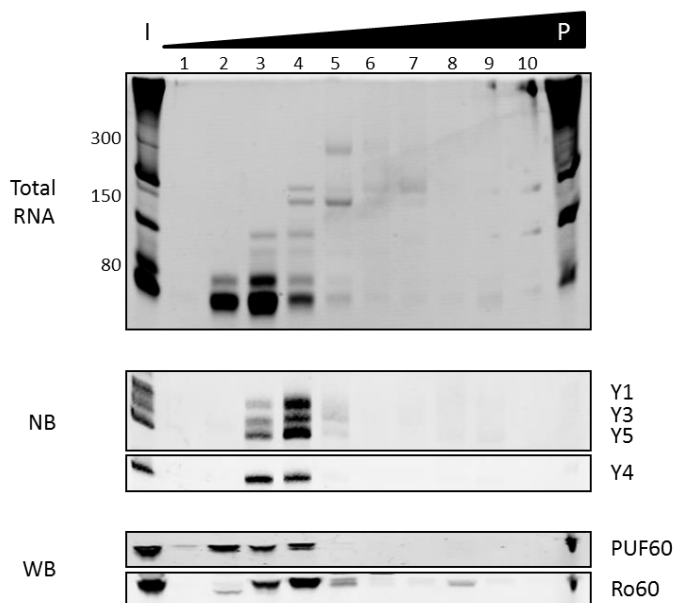


Figure 12. Characterization of Y RNPs. HEK293 cell lysates were subjected to glycerol gradient analyses (10-30 % glycerol, 17h, 130.000g). RNA and protein samples were prepared from the indicated fractions (1-10) as well as the input (I) and the sedimentation pellet (P). Total RNA was resolved on a denaturing TBE-urea gel and stained with ethidium bromide (RNA sizes (nts) are indicated on the left). Furthermore RNA samples were subjected to Northern blotting (NB). The Y RNA-

binding proteins PUF60 and Ro60 were analyzed by Western blotting (WB) of the indicated fractions (unpublished data).

*3.9. The association of Y3/Y3** with mRNA 3'-end processing factors*

Our RNA pulldown analyses revealed a multitude of potential Y RNA-binding proteins (chapter 3.5.). With the aim to characterize novel Y RNA functions we analyzed the identified Y RNA-associated proteins for their reported cellular roles. Interestingly, proteins involved in the 3'-end processing of eukaryotic mRNAs interacted with Y3 and to a lesser extent with Y1 (Köhn et al. 2015 Figure 1). Since Y RNAs had never been associated with the 3'-end maturation of mRNAs we studied the interaction with these processing factors in further detail.

The 3'-end processing of mRNAs in mammals essentially relies on *cis*-determinants within the 3'-UTRs of the respective transcripts. Distinct multi-protein complexes were reported to associate with these determinants to finally guide the 3'-end maturation of eukaryotic mRNAs. Up to now two major processing pathways have been identified, a specialized pathway for replication-dependent histone mRNAs and one for the majority of 'conventional' mRNAs (reviewed in [72, 73]).

Conventional 3'-end processing of mRNAs essentially relies on the polyadenylation signal (PAS). This sequence (usually AAUAAA or close variants) is located within the 3'-UTR of mRNAs upstream of the cleavage site (reviewed in [72]). The PAS is bound by a protein complex called the cleavage and polyadenylation specificity factor (CPSF). The mammalian CPSF complex is composed of at least six proteins (CPSF1, CPSF2, CPSF3, CPSF4, FIP1L1 and WDR33) and associates with the PAS [74, 75]. Recent studies suggest that CPSF4 and WDR33 directly bind the PAS, which then triggers the association of other CPSF subunits [76, 77]. The CPSF complex guides the cleavage of pre-mRNAs 15-30nts downstream of the PAS (usually after a CA-dinucleotide). Cleavage is facilitated by the nuclease CPSF3 [78]. After cleavage of the mRNA the associated poly-A-polymerase synthesizes the poly-A-tail that is essential for various aspects of the mRNA life cycle (e.g. stability, nuclear export, translation). The processing efficiency is enhanced by additional *cis*-elements surrounding the PAS. The upstream sequence element (USE) for example is bound by the mammalian cleavage factor I (CFIm). The downstream sequence element (DSE) on the other hand is associated with the cleavage stimulatory factor (CSTF). Both factors were shown to be essential for efficient 3'-end formation of mammalian mRNAs [79, 80].

The 3'-UTR of mammalian replication-dependent histone mRNAs differs significantly from that of 'conventional' mRNAs. Histone mRNAs are usually not spliced and have a short 3'-UTR containing a conserved stem-loop element (SL; reviewed in [73]). The SL is bound by the stem-loop binding protein (SLBP), which influences all aspects of the histone mRNA life cycle (3'-end processing, nuclear export, translation; [81, 82]). Furthermore, histone mRNAs contain a histone downstream element

(HDE) located right after the cleavage site. This serves as binding site for the U7-snRNP [83]. CPSF was shown to associate with histone mRNAs and to act in concert with the U7-snRNP and SLBP to promote the cleavage of nascent histone transcripts [84]. Interestingly correctly processed histone mRNAs end right after the SL and in contrast to conventional mRNAs are not polyadenylated (reviewed in [73]). However, when normal histone mRNA processing is inhibited, the 3'-end processing machinery utilizes cryptic polyadenylation signals downstream of the SL leading to misprocessed and polyadenylated histone mRNAs.

In our attempts to identify novel Y RNA-associated proteins we found a variety of mRNA processing factors to associate with these ncRNAs. This included the whole set of CPSF-proteins, the CFIm and associated proteins like WDR33 as well as symplekin (Figure 13). All these proteins associated primarily with Y3 and to a lesser extent with Y1 as demonstrated by mass spectrometry.

Protein (Gene Symbol)	C	Y1	Y3	Y4	Y5	
Core CPSF	CPSF160 (CPSF1)		4,3 6	11,4 16		
	CPSF100 (CPSF2)		1,7 1	16,1 10		
	CPSF73 (CPSF3)			5,3 3		
	CPSF30 (CPSF4)			14,1 3		
CFIm	hFIP1 (FIP1L1)		2,9 1	14,8 7		
	CFIm25 (CPSF5)	6,6 1	38,8 10	45,8 13		14,5 2
	CFIm68 (CPSF6)		9,6 4	16,5 9	4,5 1	4,5 1
Scaffold	CFIm59 (CPSF7)		14,4 5	16,8 9		
	WDR33			11,0 13		
	Symplekin (SYMPK)		2,2 2	4,1 4		

Figure 13. Y RNAs associate with processing factors.

Proteins co-purified with Y RNAs by RNA pulldowns were analyzed by mass spectrometry. This revealed the association with proteins involved in the 3'-end processing of mRNAs. The peptide coverage (PC: blue) and the peptide spectral matches (PSMs: red) are depicted for the respective proteins within the different pulldown samples (taken from Köhn et al. 2015 Figure S1).

XX: Peptide coverage (PC) in %
 XX: Peptide spectral matches (PSMs)

Western blotting confirmed the association of 3'-end processing factors identified by MS analyses (Figure 14). To identify the binding site of these proteins in Y3, we explored association with truncated Y3 mutant RNAs by RNA pulldown analyses. This revealed that the uridine rich sequence within the Y3 loop is critical for the interaction of the CPSF with Y3 (see Köhn et al. 2015 Figure 1). Notably, although significantly shorter than its precursor, the identified binding motif of CPSFs is retained in the Y3** ncRNA. Accordingly, we also analyzed the association of this RNA with the CPSF complex. As expected, we observed that Y3** associates with processing factors in a U-rich element dependent manner (Figure 14).

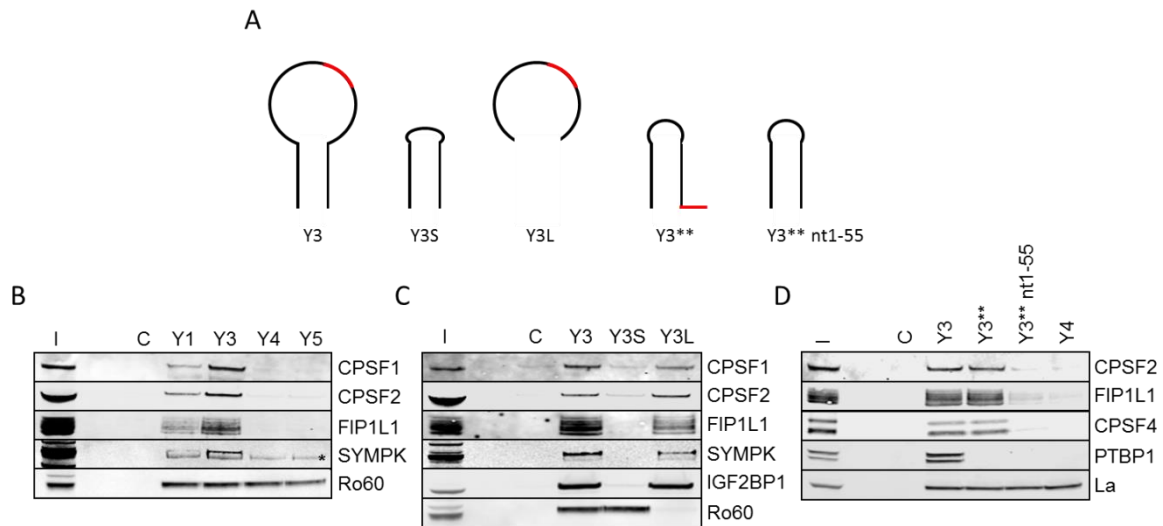


Figure 14. Characterization of the Y RNA-CPSF association. Y RNA pulldowns were performed in HEK293 cell lysates and associated proteins were analyzed by Western blotting, as described in chapter 3.5. (A) Schematic of Y3, Y3** and the mutants used in RNA pulldown analyses. The U-rich element is colored in red. (B) The association of CPSF1, CPSF2, FIP1L1 and SYMPK with all four human Y RNAs was analyzed by RNA pulldowns in HEK293 cell lysates. Ro60-binding served as positive control. The asterisk indicates a cross reaction of the SYMPK-antibody. The lysate input fraction is indicated by (I) and beads alone (C) served as negative control. (C) Y3 fragments were analyzed for processing factor association by RNA pulldowns. In addition to Y3, the Y3-stem (Y3S) and the Y3-loop (Y3L) were used in these studies. Ro60 (stem-associated; [24]) and IGF2BP1 (loop-associated; [58]) served as positive controls for Y3S and Y3L, respectively. (D) Y3** association with processing factors was analyzed by RNA pulldown analyses in HEK293 cell lysates. Next to full length Y3, Y3** and a Y3** mutant lacking the CPSF binding motif (nt1-55) were analyzed. Y4 served as negative control. PTBP1 association served as an Y3-specific positive control. The co-purification of La indicated association with the 3'-end of Y RNAs (taken from Köhn et al. 2015 Figure 1, 4 and S1).

In summary we identified the association of Y3, Y3** and Y1 with proteins involved in the 3'-end processing of mRNAs. This interaction might be mediated by the direct binding of FIP1L1 and concomitant association of CPSF4, which then recruit additional processing factors to Y RNAs (see Köhn et al. 2015 Figure 4 and S3). FIP1L1 and CPSF4 were already shown to preferentially bind U-rich RNAs, a finding which is supported by our analyses [75, 85]. The interaction of Y RNAs with processing factors raised the question, if these ncRNAs could be associated with the 3'-end processing of mRNAs. Indeed we could show an involvement of Y3/Y3** in the processing of replication-dependent histone mRNAs. These findings are further discussed in chapter 5.

4. Y RNA functions

For a long time the cellular functions of small non-coding Y RNAs remained elusive. Within the past few years some progress was made to elucidate some roles these ncRNAs may serve. However, most of these findings are limited to bacteria. In the following, the roles identified for Y RNAs in higher mammals and bacteria are discussed.

4.1. *The role of Y RNAs in DNA replication and cell growth*

Isolated late-G1-phase nuclei maintain their capability for DNA replication, but replication can be stimulated by the addition of cytosolic extracts. In an attempt to identify the stimulatory molecules within these cytosolic extracts, Y RNAs were found to greatly enhance replication in this *in vitro* system [86]. This function was furthermore described to be fulfilled by all four human Y RNAs and critically depends on a sequence motif present within the double-stranded stem of Y RNAs [87]. It was further proposed that the stimulatory effect of Y RNAs on DNA replication occurs at the initiation step of replication [88]. Along these lines it was suggested that Y RNAs physically interact with chromatin, an interaction which could also occur indirectly by Y RNA-associated proteins, for instance the origin recognition complex [89]. The interaction of Y RNAs with Ro60, La and Nucleolin on the other hand is not essential for their function in DNA replication [90]. The depletion of Y1 and Y3 by siRNAs in human cells reduced the number of mitotic cells, but had no significant impact on cell death [91]. Furthermore the inhibition of Y RNAs by morpholino oligos in *X. laevis* and *D. rerio* is lethal around the midblastula transition in embryonic development, which was correlated with an increased rate of DNA replication during this embryonic stage [92].

Replication-dependent histone mRNA levels are very sensitive to changes of the replication rate. Thus, histone mRNAs are rapidly degraded when DNA replication is inhibited [93]. To test if the depletion of Y RNAs results in altered total histone mRNA abundance, we performed Y RNA knockdown studies in human cells and determined the amount of total cellular histone mRNAs (see chapter 5). However, we did not observe any significant changes in total histone mRNA abundances upon Y RNA depletion (Figure 16). Notably, total histone mRNAs remained unaffected no matter how Y RNAs were depleted (siRNAs via the RISC or ASOs via RNase H). Furthermore, we could not identify any protein of the origin recognition complex to associate with Y RNAs in RNA pulldowns (see Köhn et al. 2015 Table S1). Thus, at present we have no evidence supporting a role of Y RNAs in DNA replication. However, we observed that Y RNAs modulate cell growth or viability (Figure 15). ASOs targeting Y1, Y3, Y4 and the unrelated U7 snRNA were transfected into cells, which were then analyzed for cell growth after 48h with a cell viability assay. The depletion of Y1 and Y3 by ASOs severely impaired cell viability 48h post transfection. In contrast, cell viability appeared essentially

unchanged by the ASO-directed knockdown of Y4, U7 or the transfection of control ASOs. Similar results were obtained by ASO-mediated Y RNA depletion in other human cell lines (data not shown). Thus, we concluded that at least Y1 and Y3 are essential to maintain or enhance the viability of human cells.

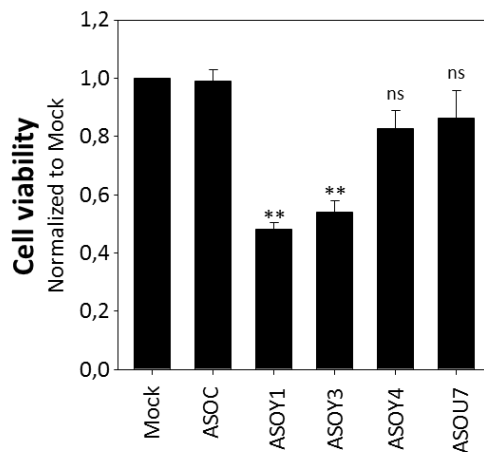


Figure 15. The impact of Y RNA depletion on cell growth. HEK293 cells were transfected with ASOs targeting Y1, Y3, Y4 and U7. After 48h the cells were harvested and analyzed by cell titer blue assay according to manufacturer's protocols (Promega). Cell viability is depicted relative to mock-transfected controls (Student's t-test: $p^{**}<0,01$, ns – not significant; $n=3$; unpublished data).

4.2. Y RNAs as modulators of Ro60 function and cellular stress

In addition to Y RNAs, mammalian Ro60 was reported to bind small misfolded ncRNAs such as 5S rRNA or U2 snRNA [94, 95]. The Ro60 crystal structure in complex with 5S or Y RNA fragments suggested that binding to these RNA substrates presumably is mutually exclusive [32]. Therefore it was proposed that Y RNAs might compete with misfolded RNAs for binding to Ro60. However, it remains to be elucidated if this competition is physiological relevant in mammalian cells. Furthermore, Y RNA-binding can influence the localization of the Ro60 protein in mammalian cells. Ro60 is localized in both the nucleus and the cytoplasm under normal cellular conditions, but accumulates in nuclei upon stress conditions, for instance in response to UV-irradiation [96]. Interestingly a Ro60 mutant incapable of Y RNA-binding strongly accumulates in nuclei under normal growth conditions [96]. This suggests that Y RNAs are involved in the nucleo-cytoplasmic transport of Ro60. In support of this it was shown that complexes consisting of Ro60, Y3 and IGF2BP1 are exported to the cytoplasm in an Exportin 1-dependent manner [70].

In autoimmune diseases such as cardiac neonatal lupus (NL) the Ro60 protein is exposed on the cell surface of apoptotic cells and can trigger an autoimmune response. This can be associated with heart block and cardiomyopathy in offspring. To identify the underlying mechanisms of the cell surface exposure of Ro60, fibroblasts were analyzed for their ability to translocate cellular Ro60 to the cell surface upon apoptotic conditions [97]. These analyses showed that a Ro60 mutant defective in Y RNA-binding does not localize to the cell surface upon apoptotic conditions. Furthermore cell surface exposure of wt Ro60 is also impaired upon Y3 but not Y1 depletion. These results suggest that the binding of Ro60 to Y3 ncRNA is essential for Ro60 to be exposed on apoptotic cell surfaces

and to trigger a TLR-dependent inflammation cascade in neonatal lupus and potentially also in other autoimmune diseases involving Ro60 [97].

Bacterial Ro60 (Ro sixty related – Rsr) and associated Y RNAs were first described in *D. radiodurans* [35]. In this bacterium Rsr is expressed in low amounts at normal conditions, but is substantially induced upon UV irradiation. Moreover at least two Y RNAs have been reported in *D. radiodurans*, both of which are bound by Rsr and upregulated in response to UV irradiation [35, 98]. Like in mammalian cells bacterial Ro60 stabilizes Y RNAs since the knockout of Rsr caused a severe reduction of Y RNA levels [35]. Interestingly, the concomitant depletion of Rsr and Y RNAs led to an increased UV sensitivity compared to the parental strain [35]. These results suggest that Rsr/Y RNAs are important regulators of cell survival under stress condition such as UV stress. In *D. radiodurans* the maturation of the 23S rRNA is inefficient under normal growth conditions leading to the accumulation of 23S that contains extensions at the 5'- and 3'-end [99]. In contrast at elevated temperature 23S maturation is efficient. This increased processing efficiency at high temperatures depends on Rsr and the nucleases RNase PH/RNase II suggesting that bacterial Ro60 is involved in rRNA maturation [99]. Surprisingly Y RNA depletion leads to an efficient 23S rRNA maturation at low and high temperatures. These results suggest that bacterial Y RNAs inhibit the function of Rsr in 23S maturation at least under normal growth conditions [99]. Upon starvation in *D. radiodurans* Rsr, presumably acting together with the PNPase nuclease, is essential for the increased general RNA decay [100]. It was shown that Rsr, Y RNA and PNPase form a complex called RYPER (Ro60/Y RNA/PNPase Exoribonuclease RNP), which assembles into a structure similar to the eukaryotic exosome [101]. RYPER specializes the PNPase to degrade structured RNAs such as 23S or 16S rRNAs. The structure of RYPER determined by single-particle electron microscopy revealed that the Y RNA acts as tethering factor in RYPER connecting Rsr and the PNPase [101]. Taken together these findings provide strong evidence that bacterial Ro60 and the associated Y RNAs act as modulators of cellular RNA fate (processing and decay) especially upon stress conditions such as UV stress, starvation or heat stress. Interestingly, also the mammalian Ro60 protein promotes cell survival upon UV irradiation [95]. Future studies will have to reveal if mammalian Ro60 also influences cellular RNA degradation/processing under normal or stress conditions and how Y RNAs contribute to these functions.

5. The role of Y3/Y3 in the 3'-end processing of histone mRNAs**

5.1. The depletion of Y RNAs and their impact on pre-mRNA processing

Our analyses of Y RNA-associated proteins revealed an association with mRNA 3'-end processing factors (see chapter 3.9). To analyze if this association indicated a role of Y1 and/or Y3 in the control of mRNA processing, we analyzed mRNA 3'-end formation in human cells. To knockdown Y RNAs we used chimeric antisense oligonucleotides (ASOs). This allowed the depletion by a RISC-independent mechanism relying on RNase H mediated cleavage of endogenous RNA substrates [102, 103]. In contrast to the RISC, RNase H is present in the cytoplasm and the nucleus. Accordingly, we assumed that ASO-mediated ncRNA depletion could efficiently deplete ncRNAs from both compartments. As expected, we were able to successfully reduce the levels of Y1, Y3 and Y4 (see Köhn et al. 2015 Figure 2). So far, we failed to knockdown Y5 for unknown reasons.

If Y RNAs serve a role in the processing of mRNAs was initially analyzed by the qRT-PCR based quantification of pre-mRNA levels. We expected that misprocessed pre-mRNAs accumulate upon Y RNA depletion if these ncRNAs serve a role in either the 3'-end processing of 'conventional' mRNAs and/or canonical histone transcripts. To detect pre-mRNAs, we designed PCR-primers allowing the amplification of misprocessed as well as total mRNAs. At first we focused on replication-dependent (canonical) histone mRNAs, since we had established knockdown protocols for the U7 ncRNA which is essential for the 3'-end processing of histone transcripts (Figure 16; [102, 104]). These analyses revealed that the depletion of Y3 and to a lesser extent Y1 led to a significant increase of misprocessed H2AC and H3A histone mRNAs. As expected, the depletion of U7 also caused a significant accumulation of misprocessed histone mRNAs as well. Notably, this was not observed upon the knockdown of Y4. The latter was expected to serve as negative control since it was not associated with RNA processing factors (see Figure 14). In contrast to the abundance of misprocessed transcripts, total levels of histone mRNAs remained essentially unchanged upon depletion of Y RNAs as well as U7 snRNA. Together this provided strong evidence for a role of Y1 and Y3 in the 3'-end processing of canonical histone transcripts. Unlike most mRNAs, correctly processed histone mRNAs are not polyadenylated. However, misprocessed histone mRNAs utilize downstream polyadenylation signals and are polyadenylated. Consistently, we confirmed that the misprocessed histone mRNAs which accumulate upon Y1, Y3 or U7 depletion are also polyadenylated by using dT-priming/qRT-PCR (see Köhn et al. 2015 Figure 2). To analyze if the depletion of Y3 also affects the processing of 'conventional' mRNAs was initially investigated by monitoring 3'-end misprocessing of the ACTB and EEF2 pre-mRNAs (Figure 16). For these studies the depletion of CPSF1 by siRNAs served as positive control, since this protein is essential for all 3'-end processing pathways. Strikingly, the processing as

The role of Y3/Y3** in the 3'-end processing of histone mRNAs

well as the total abundance of both mRNAs appeared essentially unaffected by the depletion of Y3 but processing was significantly impaired by the knockdown of CPSF1, as expected. These studies suggested that Y1 and Y3 modulate the 3'-end processing of canonical histone mRNAs but not 'conventional' mRNAs.

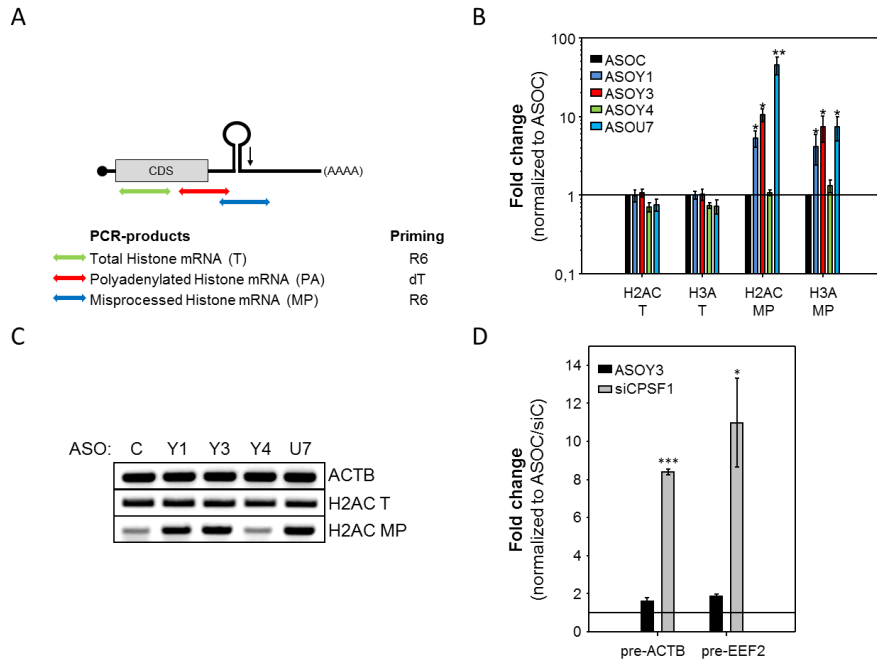


Figure 16. The influence of Y RNA depletion on pre-mRNA processing. (A) PCR-strategy for the detection of histone mRNA variants by qRT-PCR. For total and misprocessed histone mRNAs cDNAs were synthesized using random primers (R6). Polyadenylated histone mRNAs were detected by dT-priming. The obtained PCR-products are depicted by colored arrows and the cleavage sites in analyzed histone mRNAs are indicated by a black arrow. (B) Control (ASOC) or ncRNA targeting ASOs (ASOY1, ASOY3, ASOY4, ASOU7) were transfected into HEK293 cells. Total cellular RNA was extracted 48h post transfection and subjected to qRT-PCR analyses. The levels of total (T) as well as misprocessed (MP) pre-mRNAs (H2AC: HIST1H2AC; H3A: HIST2H3A) were determined relative to controls transfected with control ASOs (ASOC). Note that polyadenylated histone mRNAs showed a similar accumulation upon Y1, Y3 and U7 knockdowns (see Köhn et al. 2015 Figure 2). (C) Samples studied in (B) were analyzed by semi-quantitative RT-PCR analyses. PCR-products representing total (T) and misprocessed (MP) H2AC mRNAs were resolved on an agarose gel and stained by ethidium bromide. ACTB mRNA served as loading control. (D) The levels of pre-ACTB and pre-EEF2 mRNAs were quantified as in (B) upon the depletion of Y3 by ASOs or CPSF1 by siRNAs, respectively. All mRNA levels were normalized by the $\Delta\Delta C_t$ -method using ACTB and PPIA mRNAs as references. Asterisks indicate significant changes (Student's t-test: $p^* < 0,05$; $p^{**} < 0,01$; $p^{***} < 0,001$; $n \geq 3$; taken from Köhn et al. 2015 Figure 2 and S2).

*The role of Y3/Y3** in the 3'-end processing of histone mRNAs*

Aiming to investigate defects in 3'-end processing at genome wide scale, we analyzed how the depletion of Y3 or U7 affects pre-mRNA processing using RNA sequencing (RNA seq). To this end, total RNA isolated from ASO-transfected HEK293 cells (ASOC, ASOY3 and ASOU7; Figure 17) were subjected to the depletion of ribosomal RNA, heat fragmentation and random-primed cDNA synthesis. Barcoded cDNA libraries were then subjected to RNA seq using an Illumina HiScan-SQ sequencer. The resulting reads were aligned to the human genome using Bowtie 2 and analyzed by the DNASTAR Lasergene software package and SeqMonk. These analyses allowed the identification of 46 distinct histone mRNAs in HEK293 cells. To analyze how the depletion of ncRNAs affects the 3'-end processing of specific transcripts, the sequence reads of histone mRNAs were collapsed to the conserved histone mRNA cleavage site downstream of the stem-loop (indicated as '0'). As expected the sequencing coverage of histone mRNAs dramatically decreased at the cleavage site indicating efficient 3'-end processing and low levels of misprocessed histone mRNAs under control conditions (ASOC). In contrast, the read coverage downstream of the cleavage site was significantly increased by the depletion of U7 or Y3 indicating misprocessing at the 3'-end. Notably, the sequencing coverage 5' of the cleavage site remained essential unchanged upon the depletion of either U7 or Y3 indicating that the total abundance of histone mRNAs remained unaffected. This supported the PCR-based studies (see Figure 16). To evaluate if the depletion of U7 and/or Y3 also affects the 3'-end processing of 'conventional' non-histone mRNAs, we analyzed the 3'-sequencing coverage for eight mRNAs: ACTB, ACTG1, EEF2, GAPDH, RPL8, RPL29, RPS2, and PPIB. In these studies the polyadenylation signal (PAS) was chosen as an anchor to collapse the accumulated sequence reads of the eight reference mRNAs (Figure 17B). Consistent with efficient cleavage 10-20 nucleotides downstream of the PAS (reviewed in [105]), the 3'-sequencing coverages essentially dropped to zero. However, the accumulated sequencing coverages were indistinguishable for all three sets of samples indicating that the depletion of either U7 or Y3 did not impair the 3'-end processing of the analyzed mRNAs. These findings supported the PCR-based studies and strongly suggest that the depletion of Y3 has no general effect on the 3'-end processing of mRNAs but specifically modulates the 3'-end processing of canonical histone pre-mRNAs.

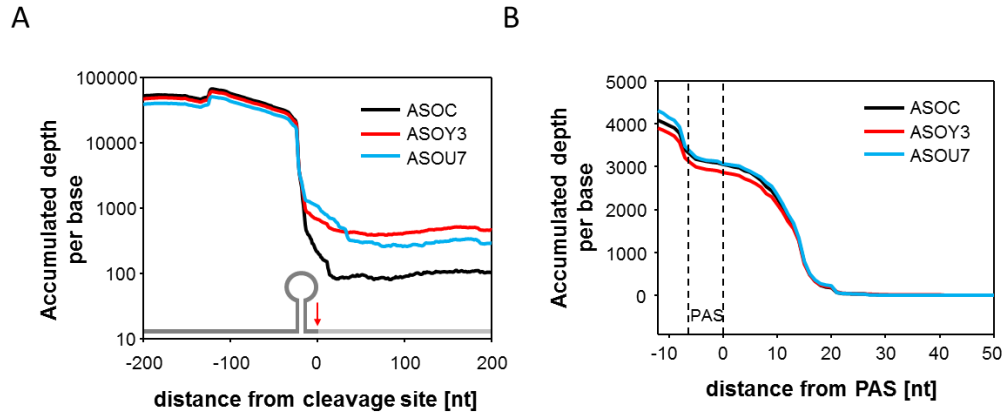


Figure 17. Transcriptome wide analysis of mRNA processing. RNA seq was conducted to analyze changes in the 3'-end processing of mRNAs. For these studies three independent total RNA samples derived from HEK293 cells transfected with either control ASOs (ASOC, black), Y3-directed ASOs (ASOY3, red) or U7-targeting ASOs (ASOU7, blue) were analyzed by the NGS-Facility of the IZKF in Leipzig. (A) For 46 histone mRNAs the 3'-end sequencing reads 200 nucleotides up- and down-stream of the cleavage site (indicated by the red arrow) were collapsed to indicate the accumulated depth per base. (B) The accumulated sequencing depth of eight non-histone mRNAs was analyzed from 10 nucleotides up- to 50 nucleotides down-stream of the polyadenylation signal (PAS; indicated by dashed lines) as in (A). The mean read values of the three samples analyzed per condition were used for determining the accumulated sequencing depth per base (taken from Köhn et al. 2015 Figure 6).

5.2. The evolutionary conservation of Y3's role in histone mRNA processing

The finding that the expression of Y RNAs is highly conserved suggested that their function is conserved as well, at least in higher eukaryotes. Therefore we analyzed if the depletion of Y3 in cells derived from other species than human results in an impaired processing of histone transcripts as well. Accordingly, the levels of misprocessed histone mRNAs were monitored in distinct cell lines upon the depletion of Y3 or U7 using qRT-PCR (Figure 18A). These analyses confirmed U7 as a highly conserved regulator of 3'-end processing in all analyzed cell lines, since the abundance of misprocessed transcripts increased upon its depletion (Figure 18A, grey bars). Surprisingly, the knockdown of Y3 impaired the processing of histone transcripts only in cells derived from human, monkey and guinea pig but not in cells derived from *muroidea* (mouse-like rodents), as demonstrated here for rat and mouse cells (Figure 18A, red bars). These results suggested that the function of Y3 ncRNA in histone mRNA processing is not conserved in *muroidea*. Therefore we analyzed the expression of Y RNAs by Northern blotting in a panel of cell lines derived from distinct species (Figure 18B). Consistent with previous studies, Y1 and Y3 but not Y4 and Y5 were observed in *muroidea*-derived cells [23]. However, the presence of a smaller variant of Y3, termed Y3**, which presumably is derived by nucleolytic processing of the Y3 precursor (see Köhn et al. 2015 Figure 3, 4

The role of Y3/Y3** in the 3'-end processing of histone mRNAs

and S3 for further detail) was significantly correlated with a Y3-dependent modulation of histone mRNA processing. This suggested that Y3** rather than Y3 is involved in the control of histone mRNA processing.

Up to now we can only speculate why *muroidea* derived cells lost the expression of Y3**. We assume that Y3** derives from its precursor Y3 in non-*muroidea*. Most likely a few nucleotide variations in the 5'-region of Y3 in *muroidea* lead to the selective destabilization of Y3** but not Y3 or the nucleolytic cleavage of Y3 is inhibited (see chapter 3.3.). The loss of Y3** and therefore its putative function in histone mRNA processing could be compensated by another unknown ncRNA or the assembly of processing factors at the histone pre-mRNA adapted to be not dependent on Y3** function in *muroidea*.

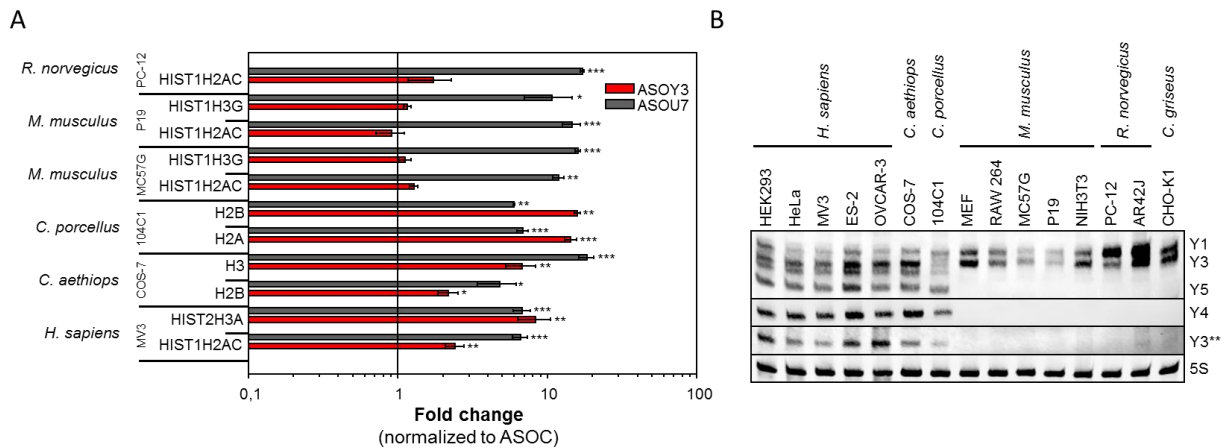


Figure 18. Conservation of the Y3 function. (A) The levels of misprocessed histone mRNAs were quantified by qRT-PCR upon depletion of Y3 or U7 RNAs, essentially as described in Figure 16. Cell lines derived from indicated species were transfected with control, Y3- or U7-directed ASOs and the abundance of indicated misprocessed histone pre-mRNAs was determined 48h post-transfection. All histone mRNA levels were normalized to ACTB/PPIA as well as ASOC transfection (Student's t-test: $p^* < 0,05$; $p^{**} < 0,01$; $p^{***} < 0,001$; $n=3$). (B) Y RNA levels were analyzed by Northern blotting of total cellular RNA isolated from respective cell lines and species (taken from Köhn et al. 2015 Figure 3).

5.3. Y3** ncRNA is essential for histone mRNA processing

The analyses of Y3's role and expression in cell lines derived from distinct species strongly suggested that Y3** instead of Y3 is essential for the processing of histone mRNAs. To test this hypothesis, we first analyzed the depletion of Y3 and Y3** by ASOs versus siRNAs of identical primary sequence in HEK293 cells. Surprisingly, we observed that ASOs depleted both, Y3 and Y3**, whereas siRNAs only reduced the abundance of Y3 (Figure 19A). This could be due to the different silencing mechanisms used by these antisense molecules (ASO: RNase H vs. siRNA: RISC). Irrespective of the exact mechanism, these studies allowed us to test for an Y3**-dependent regulation of histone pre-mRNA

*The role of Y3/Y3** in the 3'-end processing of histone mRNAs*

processing. Accordingly, we monitored misprocessing of selected histone transcripts upon the depletion of both Y3/Y3** (by ASOs) versus the sole knockdown of Y3 (by siRNAs) using qRT-PCR (Figure 19B). These studies clearly demonstrated that the processing of histone transcripts was only affected by the concomitant depletion of Y3 and Y3** but remained essentially unchanged by the knockdown of Y3. Although these findings alone do not rule out that Y3 serves a role in the 3'-end processing of histone pre-mRNAs this strongly support the notion that Y3** is essential. This is furthermore supported by ASO-directed depletion of Y3 in cells lacking Y3** (see Figure 18).

In line with our findings, it remained to be determined if Y3** and/or Y3 also associate with histone mRNAs. To investigate this we performed RNA pulldowns using immobilized biotinylated Y3 or Y3** RNAs in HEK293 cell lysates and monitored the co-purification of endogenous mRNAs by qRT-PCR (Figure 19C). These analyses revealed that histone mRNAs selectively associate with Y3**, whereas other mRNAs (RPS6 and HSPA5) were not efficiently co-purified. In contrast, barely any association of the tested mRNAs was observed for Y3. This supported the view that Y3** is essential for the processing of histone transcripts and associated with the latter.

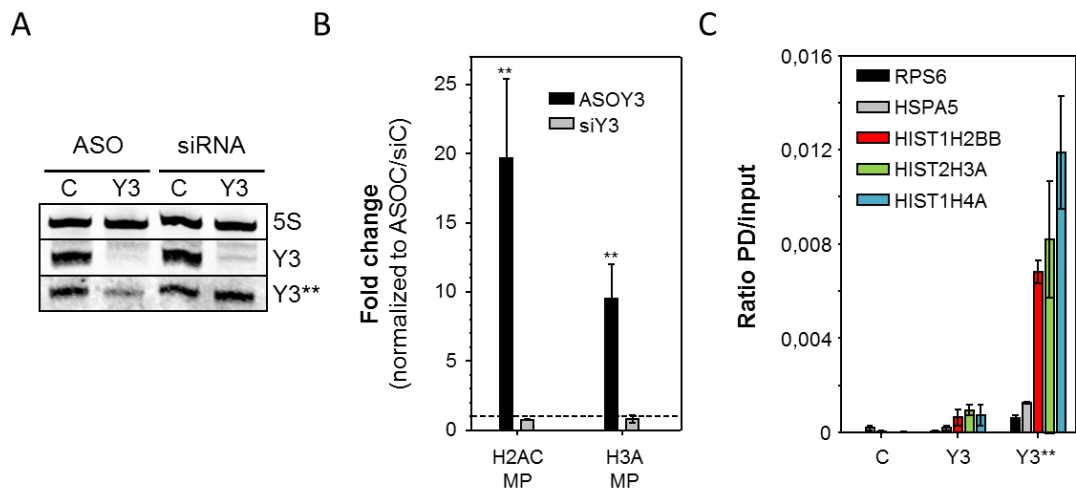


Figure 19. The role of Y3 in histone mRNA processing.** (A) HEK293 cells were transfected with ASOC and ASOY3 as well as siC and siY3. Total RNA was extracted 48h post transfection and subjected to Northern blotting to detect ncRNAs (Y3, Y3** and 5S as loading control). (B) Samples from (A) were analyzed by qRT-PCR to determine the levels of misprocessed histone mRNAs (H2AC and H3A). The histone mRNA levels were normalized to ACTB/PPIA and to the respective control sample (ASOC or siC; Student's t-test: $p^{**} < 0,01$; $n=3$). (C) RNA pulldowns were performed with beads only (C) as well as biotinylated Y3 and Y3** RNAs. Associated RNAs were isolated from the respective pulldowns and analyzed by qRT-PCR. The ratio between pulldown and input samples was calculated with the ΔC_t -method ($n=3$; taken from Köhn et al. 2015 Figure 3 and 4).

The role of Y3/Y3** in the 3'-end processing of histone mRNAs

To map the *cis*-determinants mediating the association of Y3** with histone transcripts, we performed RNA pulldown analyses (Figure 20). Therefore we immobilized biotinylated RNA fragments spanning the coding sequence and the 3'-UTR of the HIST2H3A mRNA. RNA pulldowns were performed in HEK293-lysate supplemented with Atto680-labeled Y3** RNA. The immobilized as well as co-purified RNAs were analyzed by gel electrophoresis and detected by Syto60-staining (bait RNAs) or infrared imaging (Atto680-labeled Y3**). Strikingly, Y3** clearly associated with histone RNA fragment 4 comprising parts of the coding sequence as well as the complete 3'-UTR of the HIST2H3A transcript. Notably, any further 3'-shortening of fragment 4 abolished the association indicating Y3** associates at the very 3'-part of this HIST2H3A transcript. Interestingly this region comprises the conserved histone downstream element (HDE), where the U7 snRNA interacts with histone mRNAs to guide histone mRNA processing [83]. Taken together our studies confirm the association of Y3** with histone mRNAs and suggest that Y3**'s role in histone mRNA processing could be mediated by an association with histone mRNAs near the HDE element.

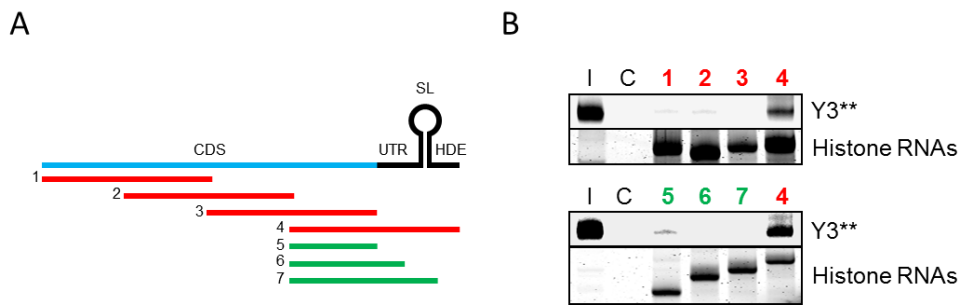


Figure 20. The association of Y3 with histone RNAs.** (A) RNA pulldowns were performed with indicated overlapping biotinylated fragments of the human HIST2H3A transcript (fragments 1-7). Fragments 1, 2 and 3 covered the coding sequence (CDS) of the histone mRNA. Fragment 4 included parts of the CDS as well as the 3'-untranslated region (UTR), the stem-loop (SL) and the histone downstream element (HDE). Fragments 5-7 are 3'-truncated RNAs of fragment 4 and were used to further map the Y3** association. (B) Eluted RNAs derived by RNA pulldowns, indicated by the respective numbers, together with control pulldowns (C) and input RNA (I) were resolved on TBE-urea gels. Gels were imaged by infrared scanning to determine Atto680-labeled Y3**. The latter was added to HEK293 cell lysates prior to pulldown analyses. Finally, gels were stained with Syto60 to detect the bait histone RNA fragments.

It should be noted, that the ASO-mediated depletion of Y1 in human cells led to the accumulation of misprocessed histone mRNAs as well (see Figure 16). Y1 and Y3 ncRNAs are very similar and the U-rich sequence important for Y3** production is partially conserved in Y1. In support of this we could identify a smaller variant of Y1 upon the overexpression of the Y1 gene in human cells by Northern blotting (data not shown). This ncRNA in principle could function similar to the Y3**

*The role of Y3/Y3** in the 3'-end processing of histone mRNAs*

RNA. For now we did not investigate this in further detail, since Y3** appeared more effective in histone mRNA processing and endogenous 'Y1**' levels are very low at steady state, at least in HEK293 cells.

*5.4. Y3** ncRNA promotes integrity and dynamics of histone locus bodies*

The genes encoding for the major histone proteins (H2A, H2B, H3, H4 and H1) are arranged in genomic clusters in higher eukaryotes. In human, most histone proteins are encoded from multiple distinct genes. These are mainly organized in two genomic clusters on chromosomes one and six. It is presumed that this genomic organization is essential for the tight temporal control of histone expression in so called 'transcription factories' (reviewed in [106] and [107]). Remarkably, these 'factories' are even visible as discrete nuclear foci by fluorescence microscopy and were termed histone locus bodies (HLBs). Thus, HLBs are assumed to indicate discrete sites of histone mRNA synthesis and the 3'-end processing of nascent histone transcripts, as evidenced by the accumulation of transcription and processing factors at HLBs [108, 109]. Histone mRNA synthesis is tightly controlled during the cell cycle with a sharp increase of histone synthesis during S-phase when DNA is replicated and has to be packed into nucleosomes [110]. Histone transcription factors like NPAT and 3'-end processing factors (like FLASH) are enriched in HLBs and are also used as HLB marker proteins [111]. Interestingly, NPAT is associated with histone loci already in the G1-phase of the cell cycle, but is activated by phosphorylation selectively in S-phase. Due to the activation by cyclin dependent kinases (CDKs), NPAT promotes histone mRNA synthesis and subsequent processing of the histone transcripts [112].

The depletion of Y3/Y3** as well as the U7 ncRNAs impaired histone pre-mRNA processing, whereas overall synthesis of histone transcripts appeared unaffected (chapter 5.1.). We aimed at analyzing if HLB morphology and/or the recruitment of processing factors are impaired by the depletion of ncRNAs regulating the 3'-end processing of histone pre-mRNAs. To this end, we performed ncRNA knockdown analyses in human melanoma-derived MV3 cells, since these cells are suitable for imaging and also showed an increase of misprocessed histone mRNAs upon Y3/Y3** depletion (Figure 18, Figure 21). HLB morphology was monitored by indirect immunostaining of NPAT and FLASH and analyzed by fluorescence microscopy. This revealed that the apparent diameter of HLBs was significantly reduced by the depletion of Y3/Y3** (ASOY3) whereas it remained essentially unchanged in response to the knockdown of U7 (Figure 21A and B). Consistently, the concomitant depletion of Y3/Y3** and U7 induced a significant reduction in HLB size as well, suggesting that the depletion of U7 cannot compensate for morphological effects induced by the depletion of Y3/Y3**. In summary these findings indicated that the depletion of Y3/Y3** is essential for the formation and/or maintenance of human HLBs suggesting a role of Y3/Y3** in the recruitment of protein

The role of Y3/Y3** in the 3'-end processing of histone mRNAs

factors to these loci. However, HLB morphology remained unaffected by the knockdown of U7 despite its essential role in the recruitment of U7-snRNP associated proteins to sites of histone mRNA synthesis and processing. This finding could be explained by the hierarchical recruitment of histone processing factors, which was suggested also in *D. melanogaster* [113]. According to this hypothesis the U7-snRNP is recruited to the histone locus body at a later time point, when the initial HLB had already been formed.

Processing factors of the CPSF complex associate with Y3 and Y3** (chapter 3.9.), which were found to be essential for the 3'-end processing of histone mRNAs. According to our hypotheses, Y3/Y3** modulate the 3'-end processing of histone transcripts by recruiting processing factors like the CPSF. Therefore we expected that the knockdown of these processing factors affects HLB morphology as well. To test this directly, some of the CPSF-associated proteins were depleted by siRNAs in MV3 cells and HLB morphology was monitored by immunostaining of NPAT and FLASH (Figure 21C). In agreement with a Y3/Y3**-CPSF dependent control of HLB morphology, the apparent diameter of these foci was significantly decreased by the knockdown of CPSF factors. We observed the strongest effect on HLB morphology (NPAT staining) upon depletion of the FLASH protein. This might indicate a pivotal role of this protein in HLB assembly and suggests that the protein serves as an architectural scaffolding factor in HLBs. In contrast, HLB morphology remained unaffected by the knockdown of proteins associated with U7 in the U7 snRNP (LSM10 and LSM11). This indicated, consistent with the depletion of the U7 ncRNA, that the U7 snRNP is dispensable for the initial control of HLB assembly/maintenance. In conclusion these findings strongly suggest that Y3/Y3** modulate the recruitment of processing factors like the CPSF to HLB and that this is essential to establish or maintain HLB morphology. In addition our studies suggest that the recruitment of processing factors to HLBs potentially precedes the recruitment of the U7 snRNP.

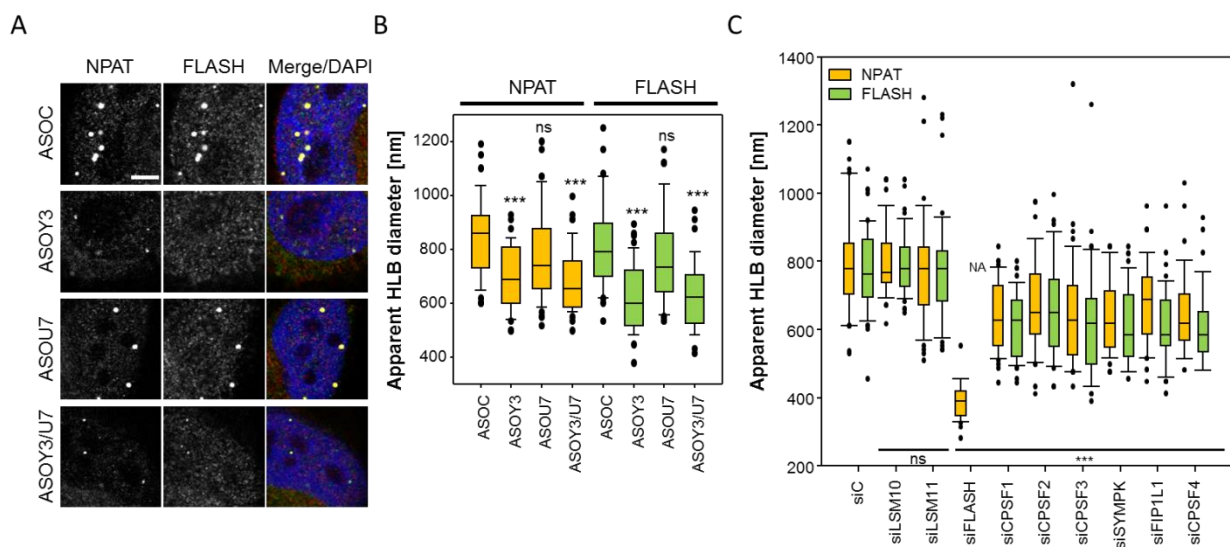


Figure 21. Influence of ncRNAs and processing factors on HLB morphology. (A) Human MV3 cells were transfected with ASOs targeting Y3/Y3**, U7 or a combination of both (ASOC served as control). HLB morphology was monitored by indirect immunostainings of NPAT and FLASH proteins revealing co-localization of both proteins in discrete nuclear foci, the HLBs. DAPI staining served as a nuclear marker. For each population a representative confocal image is shown. (B) The apparent diameters of HLBs from (A) were quantified using the Leica SP5 software. (C) RNAi was performed against proteins of the U7 snRNP (LSM10 and LSM11), processing factors (CPSF1, CPSF2, CPSF3, CPSF4, FIP1L1 and SYMPK) and FLASH. These knockdown populations were subjected to immunostainings as in (A) and quantified as in (B). The bar represents 5 μ m (Student's t-test: p***<0,001, ns – not significant, NA – not analyzed; n=35-50; taken from Köhn et al. 2015 Figure 5).

To discriminate if HLB morphology is determined by Y3 or Y3**, we first analyzed HLB morphology by ASO- versus siRNA-directed knockdowns, since the latter only deplete Y3 (see Figure 19). These studies revealed no significant change in HLB morphology by siRNA-directed depletion of Y3 and thus suggested Y3** to be essential (data not shown). To test this in further detail, we performed gain of function analyses in hamster-derived CHO cells naturally lacking Y3**. Since our NPAT and FLASH antibodies failed to detect HLBs in these cells (most likely due to species specific epitopes) we decided to establish a HLB reporter protein allowing the analysis of protein dynamics in HLBs. To this end we established a GFP-fused reporter protein called Mini-FLASH (GFP-hMF). This protein essentially lacks the central part of the FLASH protein and only contains the very N- and C-terminal domain. These are sufficient to recruit a *drosophila* FLASH mutant protein to HLBs (see Köhn et al. 2015 Figure S5; [114]). In CHO cells, lacking Y3**, GFP-hMF was co-transfected with an empty vector (control), the human Y3 gene or the Y3-T60A mutant. As described earlier (chapter 3.3.) the overexpression of the human Y3 gene leads to the synthesis of Y3 and Y3**, whereas the T60A mutant just leads to the synthesis of Y3 but not Y3**. This was also observed in CHO cells (Figure 22B). Moreover, we found that the co-expression of GFP-hMF and Y3/Y3** significantly enhanced HLB formation in CHO cells (Figure 22A). The overexpression of the mutant Y3 RNA (U60A) on the other hand did not change the size of GFP-hMF containing HLBs. In summary these findings identified GFP-hMF as a reporter protein suitable to track HLBs and provided further evidence that Y3** is essential for modulating HLB morphology.

With the GFP-hMF reporter at hand, we had a tool allowing us to study protein dynamics by FRAP (fluorescence recovery after photobleaching) in living cells. To this end, we established a stable cell line (HEK293) expressing the GFP-hMF reporter protein. As expected, the GFP-hMF protein was readily recruited to HLBs (see Köhn et al. 2015 Figure 5 and S5). Next, we determined the dynamics of the reporter protein by FRAP in cells transfected with control (ASOC) or Y3/Y3** (ASOY3) directed

*The role of Y3/Y3** in the 3'-end processing of histone mRNAs*

ASOs (Figure 22C). Single HLBs were bleached and fluorescence recovery was monitored for 90 seconds after bleaching. These analyses revealed that HLBs are dynamic nuclear bodies in which the GFP-hMF protein quickly recovers after bleaching and displays strong protein mobility, as indicated by a comparatively low immobile fraction. Upon Y3/Y3** depletion on the other hand, GFP-hMF dynamics were significantly impaired with a modestly increased half-life but significantly increased immobile fraction. In view of the fact that FLASH is considered an essential determinant of histone mRNA processing which potentially links transcription to the 3'-end processing, these findings strongly support the view that Y3** is essential for recruiting protein factors including FLASH and CPSF factors to HLBs and thus nascent histone transcripts.

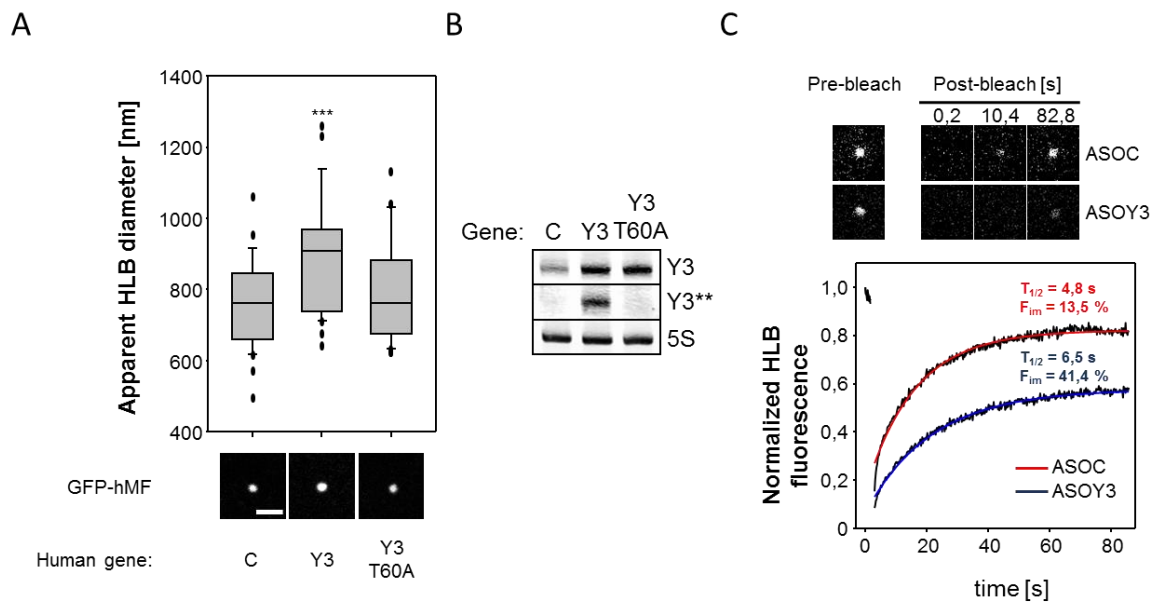


Figure 22. HLB morphology and dynamics. (A) The GFP-hMF reporter was co-expressed with an empty vector (C), the human Y3 wild type (Y3) or T60A mutant gene (Y3T60A) in hamster-derived CHO cells. HLBs were tracked by GFP-hMF and their average apparent diameters were determined with the Leica SP5 software as described in Figure 21 (bar, 3 μ m; Student's t-test: p***<0,001; n=35-50). (B) The expression of ncRNAs (Y3, Y3** and 5S as loading control) in cells from (A) was evaluated by Northern blotting. (C) FRAP experiments were conducted in HEK2993 cells stably expressing the GFP-hMF protein. Fluorescence recovery was monitored in response to the transfection of control (ASOC) or Y3/Y3**-directed ASOs (ASOY3). HLBs were bleached and fluorescence recovery was monitored in single HLBs for 90 seconds. The parameters half time of recovery ($T_{1/2}$) and immobile fraction (F_{im}) were calculated by using the raw values generated by the Leica SP5 FRAP wizard. Representative HLB images of ASOC- and ASOY3-transfected cells are shown in the upper panel before bleaching (pre-bleach) and indicated times of fluorescence recovery (n=17; taken from Köhn et al. 2015 Figure 5 and S5).

*The role of Y3/Y3** in the 3'-end processing of histone mRNAs*

In conclusion we identified, in addition to the U7 snRNA, a second ncRNA involved in the 3'-end processing of histone pre-mRNAs, the Y3** RNA (Figure 23). Like Y3, Y3** associates with mRNA 3'-end processing factors, in particular proteins of the CPSF complex. This interaction essentially relies on a U-rich sequence present in both ncRNAs. The two proteins FIP1L1/CPSF4 most likely directly associate with these ncRNAs in a cooperative manner and presumably recruit the other processing factors to small Y3** -dependent ncRNPs. We found that Y3** is likely to be processed from the Y3 ncRNA and that U60 in Y3 is critical for this processing step. Furthermore Y3**, unlike its precursor Y3, is substantially retained in the nucleus, strongly suggesting a nuclear function of this ncRNA. In fact we could show, that the concomitant depletion of Y3 and Y3** leads to the accumulation of misprocessed histone mRNAs but does not impair the processing of non-histone mRNAs. In agreement, the Y3** ncRNA selectively associates with histone mRNAs. This interaction occurs within the 3'-UTR of histone pre-mRNAs near or at the HDE. Notably, this was also proposed for the U7 snRNA. Moreover we could show that Y3** is essential for HLB integrity and protein dynamics. The depletion of processing factors by RNAi resulted in similar HLB-phenotypes suggesting that the association of Y3** with processing factors might influence the recruitment of the latter to HLBs. These results suggest a model in which Y3** associates with histone pre-mRNAs in HLBs and recruits the CPSF complex to nascent histone transcripts. These events are likely to occur before the U7 snRNP is recruited to HLBs, since neither the depletion of U7 nor the depletion of U7-associated proteins led to significant changes in HLB-morphology as assessed by NPAT and FLASH immunostainings. The Y3** -mediated processing factor recruitment however, could stimulate histone mRNA processing at the HLB, which consecutively also allows the fast synthesis of new histone proteins in the cytoplasm of cells in the S-phase. With these results we for the first time provide a model for the recruitment of the processing factors to mammalian HLBs. We propose that this is facilitated by the Y3** ncRNA recruiting the CPSF complex to nascent histone transcripts in proximity or at HLBs.

The role of Y3/Y3** in the 3'-end processing of histone mRNAs

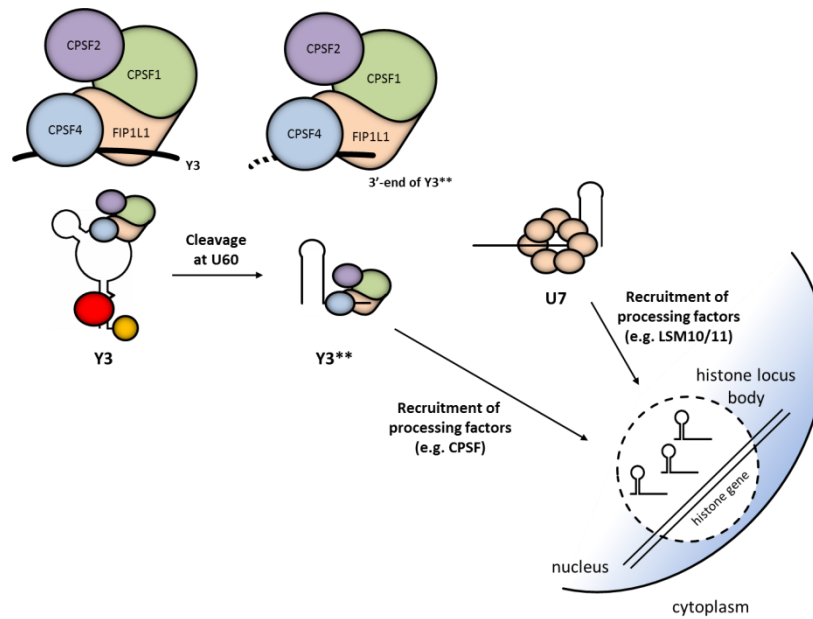


Figure 23. Proposed model of Y3's role in histone mRNA 3'-end processing.** The ncRNA Y3 as well as its truncated variant Y3** associate with mRNA processing factors like the CPSF-complex. This association is likely to be mediated by the FIP1L1 protein, which binds to the U-rich element in Y3/Y3**. In addition to the conserved function of the U7 snRNP, Y3** enhances the recruitment of mRNA processing factors to histone locus bodies (HLBs) to guide the 3'-end processing of replication dependent histone mRNAs.

Future perspective

The focus of this thesis was to investigate the cellular roles of mammalian Y RNAs. Our studies identified an essential role of Y3** in the 3'-end processing of replication-dependent histone mRNA in non-*muroides* cells. In depth analyses will have to reveal a) how Y3** is produced from its precursor Y3 b) how this processing is regulated within the cell cycle and c) which RBPs influence the synthesis of Y3** and its functions. Besides the nuclear role of Y3**, its precursor Y3 is mainly cytoplasmic at steady state. Therefore future analyses will focus on the cytoplasmic role of this ncRNA. Since we identified a multitude of cytoplasmic RBPs associating with Y3 (e.g. YBX1 or STAU1) it is tempting to speculate that Y3 could influence the functions of these RBPs by acting as decoy and/or scaffold (also see [25]).

So far we mainly focused on the roles of Y3 and Y3** in mammalian cells. Future studies may shed light on the cellular functions of Y1, Y4 and Y5 ncRNAs as well. We expect, according to their localization, Y1/Y4 could fulfill predominantly cytoplasmic and Y5 nuclear roles in mammalian cells. Our proteomic approaches, which we conducted from RNA pulldowns of all four human Y RNA family members, may give first hints towards the respective functions of these ncRNAs. Putative cellular

*The role of Y3/Y3** in the 3'-end processing of histone mRNAs*

roles could be validated by the ASO-mediated depletion or overexpression of ncRNAs. In summary, we assume that these studies will be essential to understand how ncRNAs and especially Y RNAs contribute to the complex RNA-mediated control of gene expression in mammalian cells.

References

1. Crick, F.H., *On protein synthesis*. Symp Soc Exp Biol, 1958. 12: p. 138-63.
2. Crick, F., *Central dogma of molecular biology*. Nature, 1970. 227(5258): p. 561-3.
3. Johnsson, P., et al., *Evolutionary conservation of long non-coding RNAs; sequence, structure, function*. Biochim Biophys Acta, 2014. 1840(3): p. 1063-71.
4. Jeronimo, C., et al., *Systematic analysis of the protein interaction network for the human transcription machinery reveals the identity of the 7SK capping enzyme*. Mol Cell, 2007. 27(2): p. 262-74.
5. Bogenhagen, D.F. and D.D. Brown, *Nucleotide sequences in Xenopus 5S DNA required for transcription termination*. Cell, 1981. 24(1): p. 261-70.
6. Arimbasseri, A.G., K. Rijal, and R.J. Maraia, *Transcription termination by the eukaryotic RNA polymerase III*. Biochim Biophys Acta, 2013. 1829(3-4): p. 318-30.
7. Stefano, J.E., *Purified lupus antigen La recognizes an oligouridylate stretch common to the 3' termini of RNA polymerase III transcripts*. Cell, 1984. 36(1): p. 145-54.
8. Huang, Y., et al., *Mutations in the RNA polymerase III subunit Rpc11p that decrease RNA 3' cleavage activity increase 3'-terminal oligo(U) length and La-dependent tRNA processing*. Mol Cell Biol, 2005. 25(2): p. 621-36.
9. Dieci, G., et al., *Transcription reinitiation by RNA polymerase III*. Biochim Biophys Acta, 2013. 1829(3-4): p. 331-41.
10. White, R.J., *Transcription by RNA polymerase III: more complex than we thought*. Nat Rev Genet, 2011. 12(7): p. 459-63.
11. Nikitina, T.V., L.I. Tischenko, and W.A. Schulz, *Recent insights into regulation of transcription by RNA polymerase III and the cellular functions of its transcripts*. Biol Chem, 2011. 392(5): p. 395-404.
12. Maraia, R.J., *La protein and the trafficking of nascent RNA polymerase iii transcripts*. J Cell Biol, 2001. 153(4): p. F13-8.
13. Rudt, F. and T. Pieler, *Cytoplasmic retention and nuclear import of 5S ribosomal RNA containing RNPs*. EMBO J, 1996. 15(6): p. 1383-91.
14. Maraia, R.J. and T.N. Lamichhane, *3' processing of eukaryotic precursor tRNAs*. Wiley Interdiscip Rev RNA, 2011. 2(3): p. 362-75.
15. Akopian, D., et al., *Signal recognition particle: an essential protein-targeting machine*. Annu Rev Biochem, 2013. 82: p. 693-721.
16. Bringmann, P., et al., *Evidence for the existence of snRNAs U4 and U6 in a single ribonucleoprotein complex and for their association by intermolecular base pairing*. EMBO J, 1984. 3(6): p. 1357-63.
17. Black, D.L. and A.L. Pinto, *U5 small nuclear ribonucleoprotein: RNA structure analysis and ATP-dependent interaction with U4/U6*. Mol Cell Biol, 1989. 9(8): p. 3350-9.

18. Grainger, R.J. and J.D. Beggs, *Prp8 protein: at the heart of the spliceosome*. RNA, 2005. 11(5): p. 533-57.
19. Nguyen, V.T., et al., *7SK small nuclear RNA binds to and inhibits the activity of CDK9/cyclin T complexes*. Nature, 2001. 414(6861): p. 322-5.
20. Diribarne, G. and O. Bensaude, *7SK RNA, a non-coding RNA regulating P-TEFb, a general transcription factor*. RNA Biol, 2009. 6(2): p. 122-8.
21. Lerner, M.R., et al., *Two novel classes of small ribonucleoproteins detected by antibodies associated with lupus erythematosus*. Science, 1981. 211(4480): p. 400-2.
22. Hendrick, J.P., et al., *Ro small cytoplasmic ribonucleoproteins are a subclass of La ribonucleoproteins: further characterization of the Ro and La small ribonucleoproteins from uninfected mammalian cells*. Mol Cell Biol, 1981. 1(12): p. 1138-49.
23. Wolin, S.L. and J.A. Steitz, *Genes for two small cytoplasmic Ro RNAs are adjacent and appear to be single-copy in the human genome*. Cell, 1983. 32(3): p. 735-44.
24. Wolin, S.L. and J.A. Steitz, *The Ro small cytoplasmic ribonucleoproteins: identification of the antigenic protein and its binding site on the Ro RNAs*. Proc Natl Acad Sci U S A, 1984. 81(7): p. 1996-2000.
25. Kohn, M., N. Pazaitis, and S. Huttelmaier, *Why YRNAs? About Versatile RNAs and Their Functions*. Biomolecules, 2013. 3(1): p. 143-56.
26. van Gelder, C.W., et al., *Common structural features of the Ro RNP associated hY1 and hY5 RNAs*. Nucleic Acids Res, 1994. 22(13): p. 2498-506.
27. Teunissen, S.W., et al., *Conserved features of Y RNAs: a comparison of experimentally derived secondary structures*. Nucleic Acids Res, 2000. 28(2): p. 610-9.
28. Sim, S. and S.L. Wolin, *Emerging roles for the Ro 60-kDa autoantigen in noncoding RNA metabolism*. Wiley Interdiscip Rev RNA, 2011. 2(5): p. 686-99.
29. Farris, A.D., C.A. O'Brien, and J.B. Harley, *Y3 is the most conserved small RNA component of Ro ribonucleoprotein complexes in vertebrate species*. Gene, 1995. 154(2): p. 193-8.
30. Mosig, A., et al., *Evolution of the vertebrate Y RNA cluster*. Theory Biosci, 2007. 126(1): p. 9-14.
31. Perreault, J., J.P. Perreault, and G. Boire, *Ro-associated Y RNAs in metazoans: evolution and diversification*. Mol Biol Evol, 2007. 24(8): p. 1678-89.
32. Stein, A.J., et al., *Structural insights into RNA quality control: the Ro autoantigen binds misfolded RNAs via its central cavity*. Cell, 2005. 121(4): p. 529-39.
33. Perreault, J., et al., *Retropseudogenes derived from the human Ro/SS-A autoantigen-associated hY RNAs*. Nucleic Acids Res, 2005. 33(6): p. 2032-41.
34. Boria, I., et al., *Nematode sbRNAs: homologs of vertebrate Y RNAs*. J Mol Evol, 2010. 70(4): p. 346-58.
35. Chen, X., A.M. Quinn, and S.L. Wolin, *Ro ribonucleoproteins contribute to the resistance of Deinococcus radiodurans to ultraviolet irradiation*. Genes Dev, 2000. 14(7): p. 777-82.

36. van Hoof, A., P. Lennertz, and R. Parker, *Three conserved members of the RNase D family have unique and overlapping functions in the processing of 5S, 5.8S, U4, U5, RNase MRP and RNase P RNAs in yeast*. EMBO J, 2000. 19(6): p. 1357-65.
37. Simons, F.H., et al., *The interactions with Ro60 and La differentially affect nuclear export of hY1 RNA*. RNA, 1996. 2(3): p. 264-73.
38. Garcia, E.L., et al., *Packaging of host mY RNAs by murine leukemia virus may occur early in Y RNA biogenesis*. J Virol, 2009. 83(23): p. 12526-34.
39. Gendron, M., D. Roberge, and G. Boire, *Heterogeneity of human Ro ribonucleoproteins (RNPS): nuclear retention of Ro RNPS containing the human hY5 RNA in human and mouse cells*. Clin Exp Immunol, 2001. 125(1): p. 162-8.
40. Rutjes, S.A., et al., *Rapid nucleolytic degradation of the small cytoplasmic Y RNAs during apoptosis*. J Biol Chem, 1999. 274(35): p. 24799-807.
41. Liao, J.Y., et al., *Deep sequencing of human nuclear and cytoplasmic small RNAs reveals an unexpectedly complex subcellular distribution of miRNAs and tRNA 3' trailers*. PLoS One, 2010. 5(5): p. e10563.
42. Meiri, E., et al., *Discovery of microRNAs and other small RNAs in solid tumors*. Nucleic Acids Res, 2010. 38(18): p. 6234-46.
43. Nicolas, F.E., et al., *Biogenesis of Y RNA-derived small RNAs is independent of the microRNA pathway*. FEBS Lett, 2012. 586(8): p. 1226-30.
44. Dhahbi, J.M., et al., *Deep Sequencing of Serum Small RNAs Identifies Patterns of 5' tRNA Half and YRNA Fragment Expression Associated with Breast Cancer*. Biomark Cancer, 2014. 6: p. 37-47.
45. Dhahbi, J.M., et al., *5'-YRNA fragments derived by processing of transcripts from specific YRNA genes and pseudogenes are abundant in human serum and plasma*. Physiol Genomics, 2013. 45(21): p. 990-8.
46. Gwizdek, C., et al., *Exportin-5 mediates nuclear export of minihelix-containing RNAs*. J Biol Chem, 2003. 278(8): p. 5505-8.
47. Farris, A.D., et al., *The ultrastructural localization of 60-kDa Ro protein and human cytoplasmic RNAs: association with novel electron-dense bodies*. Proc Natl Acad Sci U S A, 1997. 94(7): p. 3040-5.
48. Matera, A.G., et al., *A perinucleolar compartment contains several RNA polymerase III transcripts as well as the polypyrimidine tract-binding protein, hnRNP I*. J Cell Biol, 1995. 129(5): p. 1181-93.
49. Pollock, C. and S. Huang, *The perinucleolar compartment*. Cold Spring Harb Perspect Biol, 2010. 2(2): p. a000679.
50. Fabini, G., et al., *The heterogeneous nuclear ribonucleoproteins I and K interact with a subset of the ro ribonucleoprotein-associated Y RNAs in vitro and in vivo*. J Biol Chem, 2001. 276(23): p. 20711-8.
51. Mi, H., et al., *The PANTHER database of protein families, subfamilies, functions and pathways*. Nucleic Acids Res, 2005. 33(Database issue): p. D284-8.

52. Thomas, P.D., et al., *PANTHER: a library of protein families and subfamilies indexed by function*. Genome Res, 2003. 13(9): p. 2129-41.
53. Franceschini, F. and I. Cavazzana, *Anti-Ro/SSA and La/SSB antibodies*. Autoimmunity, 2005. 38(1): p. 55-63.
54. Wolin, S.L. and T. Cedervall, *The La protein*. Annu Rev Biochem, 2002. 71: p. 375-403.
55. Fairley, J.A., et al., *Human La is found at RNA polymerase III-transcribed genes in vivo*. Proc Natl Acad Sci U S A, 2005. 102(51): p. 18350-5.
56. Green, C.D., et al., *Binding of the 60-kDa Ro autoantigen to Y RNAs: evidence for recognition in the major groove of a conserved helix*. RNA, 1998. 4(7): p. 750-65.
57. Xue, D., et al., *A lupus-like syndrome develops in mice lacking the Ro 60-kDa protein, a major lupus autoantigen*. Proc Natl Acad Sci U S A, 2003. 100(13): p. 7503-8.
58. Wachter, K., et al., *Subcellular localization and RNP formation of IGF2BPs (IGF2 mRNA-binding proteins) is modulated by distinct RNA-binding domains*. Biol Chem, 2013. 394(8): p. 1077-90.
59. Fouraux, M.A., et al., *Nucleolin associates with a subset of the human Ro ribonucleoprotein complexes*. J Mol Biol, 2002. 320(3): p. 475-88.
60. Kohn, M., et al., *Near-infrared (NIR) dye-labeled RNAs identify binding of ZBP1 to the noncoding Y3-RNA*. RNA, 2010. 16(7): p. 1420-8.
61. Bell, J.L., et al., *Insulin-like growth factor 2 mRNA-binding proteins (IGF2BPs): post-transcriptional drivers of cancer progression?* Cell Mol Life Sci, 2013. 70(15): p. 2657-75.
62. Ross, A.F., et al., *Characterization of a beta-actin mRNA zipcode-binding protein*. Mol Cell Biol, 1997. 17(4): p. 2158-65.
63. Lawrence, J.B. and R.H. Singer, *Intracellular localization of messenger RNAs for cytoskeletal proteins*. Cell, 1986. 45(3): p. 407-15.
64. Olink-Coux, M. and P.J. Hollenbeck, *Localization and active transport of mRNA in axons of sympathetic neurons in culture*. J Neurosci, 1996. 16(4): p. 1346-58.
65. Kislauskis, E.H., X. Zhu, and R.H. Singer, *Sequences responsible for intracellular localization of beta-actin messenger RNA also affect cell phenotype*. J Cell Biol, 1994. 127(2): p. 441-51.
66. Huttelmaier, S., et al., *Spatial regulation of beta-actin translation by Src-dependent phosphorylation of ZBP1*. Nature, 2005. 438(7067): p. 512-5.
67. Runge, S., et al., *H19 RNA binds four molecules of insulin-like growth factor II mRNA-binding protein*. J Biol Chem, 2000. 275(38): p. 29562-9.
68. Hammerle, M., et al., *Posttranscriptional destabilization of the liver-specific long noncoding RNA HULC by the IGF2 mRNA-binding protein 1 (IGF2BP1)*. Hepatology, 2013. 58(5): p. 1703-12.
69. Jonson, L., et al., *Molecular composition of IMP1 ribonucleoprotein granules*. Mol Cell Proteomics, 2007. 6(5): p. 798-811.
70. Sim, S., et al., *The zipcode-binding protein ZBP1 influences the subcellular location of the Ro 60-kDa autoantigen and the noncoding Y3 RNA*. RNA, 2012. 18(1): p. 100-10.

71. Fabini, G., et al., *Analysis of the molecular composition of Ro ribonucleoprotein complexes. Identification of novel Y RNA-binding proteins.* Eur J Biochem, 2000. 267(9): p. 2778-89.
72. Chan, S., E.A. Choi, and Y. Shi, *Pre-mRNA 3'-end processing complex assembly and function.* Wiley Interdiscip Rev RNA, 2011. 2(3): p. 321-35.
73. Marzluff, W.F., E.J. Wagner, and R.J. Duronio, *Metabolism and regulation of canonical histone mRNAs: life without a poly(A) tail.* Nat Rev Genet, 2008. 9(11): p. 843-54.
74. Murthy, K.G. and J.L. Manley, *Characterization of the multisubunit cleavage-polyadenylation specificity factor from calf thymus.* J Biol Chem, 1992. 267(21): p. 14804-11.
75. Kaufmann, I., et al., *Human Fip1 is a subunit of CPSF that binds to U-rich RNA elements and stimulates poly(A) polymerase.* EMBO J, 2004. 23(3): p. 616-26.
76. Chan, S.L., et al., *CPSF30 and Wdr33 directly bind to AAUAAA in mammalian mRNA 3' processing.* Genes Dev, 2014. 28(21): p. 2370-80.
77. Schonemann, L., et al., *Reconstitution of CPSF active in polyadenylation: recognition of the polyadenylation signal by WDR33.* Genes Dev, 2014. 28(21): p. 2381-93.
78. Mandel, C.R., et al., *Polyadenylation factor CPSF-73 is the pre-mRNA 3'-end-processing endonuclease.* Nature, 2006. 444(7121): p. 953-6.
79. Ruegsegger, U., K. Beyer, and W. Keller, *Purification and characterization of human cleavage factor Im involved in the 3' end processing of messenger RNA precursors.* J Biol Chem, 1996. 271(11): p. 6107-13.
80. Gilmartin, G.M. and J.R. Nevins, *Molecular analyses of two poly(A) site-processing factors that determine the recognition and efficiency of cleavage of the pre-mRNA.* Mol Cell Biol, 1991. 11(5): p. 2432-8.
81. Wang, Z.F., et al., *The protein that binds the 3' end of histone mRNA: a novel RNA-binding protein required for histone pre-mRNA processing.* Genes Dev, 1996. 10(23): p. 3028-40.
82. Sullivan, K.D., et al., *Knockdown of SLBP results in nuclear retention of histone mRNA.* RNA, 2009. 15(3): p. 459-72.
83. Bond, U.M., T.A. Yario, and J.A. Steitz, *Multiple processing-defective mutations in a mammalian histone pre-mRNA are suppressed by compensatory changes in U7 RNA both in vivo and in vitro.* Genes Dev, 1991. 5(9): p. 1709-22.
84. Kolev, N.G. and J.A. Steitz, *Symplekin and multiple other polyadenylation factors participate in 3'-end maturation of histone mRNAs.* Genes Dev, 2005. 19(21): p. 2583-92.
85. Barabino, S.M., et al., *The 30-kD subunit of mammalian cleavage and polyadenylation specificity factor and its yeast homolog are RNA-binding zinc finger proteins.* Genes Dev, 1997. 11(13): p. 1703-16.
86. Christov, C.P., et al., *Functional requirement of noncoding Y RNAs for human chromosomal DNA replication.* Mol Cell Biol, 2006. 26(18): p. 6993-7004.
87. Gardiner, T.J., et al., *A conserved motif of vertebrate Y RNAs essential for chromosomal DNA replication.* RNA, 2009. 15(7): p. 1375-85.
88. Krude, T., et al., *Y RNA functions at the initiation step of mammalian chromosomal DNA replication.* J Cell Sci, 2009. 122(Pt 16): p. 2836-45.

89. Zhang, A.T., et al., *Dynamic interaction of Y RNAs with chromatin and initiation proteins during human DNA replication*. J Cell Sci, 2011. 124(Pt 12): p. 2058-69.
90. Langley, A.R., et al., *Ribonucleoprotein particles containing non-coding Y RNAs, Ro60, La and nucleolin are not required for Y RNA function in DNA replication*. PLoS One, 2010. 5(10): p. e13673.
91. Christov, C.P., E. Trivier, and T. Krude, *Noncoding human Y RNAs are overexpressed in tumours and required for cell proliferation*. Br J Cancer, 2008. 98(5): p. 981-8.
92. Collart, C., et al., *The midblastula transition defines the onset of Y RNA-dependent DNA replication in Xenopus laevis*. Mol Cell Biol, 2011. 31(18): p. 3857-70.
93. Borun, T.W., et al., *Further evidence of transcriptional and translational control of histone messenger RNA during the HeLa S3 cycle*. Cell, 1975. 4(1): p. 59-67.
94. Shi, H., et al., *A misfolded form of 5S rRNA is complexed with the Ro and La autoantigens*. RNA, 1996. 2(8): p. 769-84.
95. Chen, X., et al., *The Ro autoantigen binds misfolded U2 small nuclear RNAs and assists mammalian cell survival after UV irradiation*. Curr Biol, 2003. 13(24): p. 2206-11.
96. Sim, S., et al., *The subcellular distribution of an RNA quality control protein, the Ro autoantigen, is regulated by noncoding Y RNA binding*. Mol Biol Cell, 2009. 20(5): p. 1555-64.
97. Reed, J.H., et al., *Ro60 requires Y3 RNA for cell surface exposure and inflammation associated with cardiac manifestations of neonatal lupus*. J Immunol, 2013. 191(1): p. 110-6.
98. Chen, X., et al., *Bacterial noncoding Y RNAs are widespread and mimic tRNAs*. RNA, 2014. 20(11): p. 1715-24.
99. Chen, X., et al., *An ortholog of the Ro autoantigen functions in 23S rRNA maturation in D. radiodurans*. Genes Dev, 2007. 21(11): p. 1328-39.
100. Wurtmann, E.J. and S.L. Wolin, *A role for a bacterial ortholog of the Ro autoantigen in starvation-induced rRNA degradation*. Proc Natl Acad Sci U S A, 2010. 107(9): p. 4022-7.
101. Chen, X., et al., *An RNA degradation machine sculpted by Ro autoantigen and noncoding RNA*. Cell, 2013. 153(1): p. 166-77.
102. Ideue, T., et al., *Efficient oligonucleotide-mediated degradation of nuclear noncoding RNAs in mammalian cultured cells*. RNA, 2009. 15(8): p. 1578-87.
103. Liang, X.H., et al., *Efficient and specific knockdown of small non-coding RNAs in mammalian cells and in mice*. Nucleic Acids Res, 2011. 39(3): p. e13.
104. Godfrey, A.C., et al., *U7 snRNA mutations in Drosophila block histone pre-mRNA processing and disrupt oogenesis*. RNA, 2006. 12(3): p. 396-409.
105. Proudfoot, N.J., *Ending the message: poly(A) signals then and now*. Genes Dev, 2011. 25(17): p. 1770-82.
106. Nizami, Z., S. Deryusheva, and J.G. Gall, *The Cajal body and histone locus body*. Cold Spring Harb Perspect Biol, 2010. 2(7): p. a000653.
107. Liu, J.L., et al., *The Drosophila melanogaster Cajal body*. J Cell Biol, 2006. 172(6): p. 875-84.

108. Salzler, H.R., et al., *A sequence in the Drosophila H3-H4 Promoter triggers histone locus body assembly and biosynthesis of replication-coupled histone mRNAs*. Dev Cell, 2013. 24(6): p. 623-34.
109. Shevtsov, S.P. and M. Dunder, *Nucleation of nuclear bodies by RNA*. Nat Cell Biol, 2011. 13(2): p. 167-73.
110. Plumb, M., J. Stein, and G. Stein, *Coordinate regulation of multiple histone mRNAs during the cell cycle in HeLa cells*. Nucleic Acids Res, 1983. 11(8): p. 2391-410.
111. Bongiorno-Borbone, L., et al., *FLASH and NPAT positive but not Coilin positive Cajal Bodies correlate with cell ploidy*. Cell Cycle, 2008. 7(15): p. 2357-67.
112. Ghule, P.N., et al., *Cell cycle dependent phosphorylation and subnuclear organization of the histone gene regulator p220(NPAT) in human embryonic stem cells*. J Cell Physiol, 2007. 213(1): p. 9-17.
113. White, A.E., et al., *Drosophila histone locus bodies form by hierarchical recruitment of components*. J Cell Biol, 2011. 193(4): p. 677-94.
114. Burch, B.D., et al., *Interaction between FLASH and Lsm11 is essential for histone pre-mRNA processing in vivo in Drosophila*. RNA, 2011. 17(6): p. 1132-47.

Es folgen auf den Seiten 47-145 die Publikationen mit Erstautorenschaft von Marcel Köhn.

1. **Köhn M.**, Lederer M., Wächter K., Hüttelmaier S. (2010)
Near-infrared (NIR) dye-labeled RNAs identify binding of ZBP1 to the noncoding Y3-RNA.
RNA 16(7):1420-8. doi: 10.1261/rna.2152710.
2. **Köhn M.**, Pazaitis N., Hüttelmaier S. (2013)
Why Y RNAs? About Versatile RNAs and Their Functions.
Biomolecules 3(1):143-56. doi: 10.3390/biom3010143.
3. Wächter K.*, **Köhn M.***, Stöhr N., Hüttelmaier S. (2013)
Subcellular localization and RNP formation of IGF2BPs (IGF2 mRNA-binding proteins) is modulated by distinct RNA-binding domains.
Biological Chemistry 394(8):1077-90. doi: 10.1515/hsz-2013-0111.

* shared first authorship
4. **Köhn M.**, Ihling C., Sinz A., Krohn K., Hüttelmaier S. (submitted 2015)
The Y3** ncRNA promotes the 3'-end processing of canonical histone mRNAs.
Submitted to *Genes & Development*

Meanwhile published as:
Köhn M., Ihling C., Sinz A., Krohn K., Hüttelmaier S. (2015)
The Y3** ncRNA promotes the 3'-end processing of histone mRNAs.
Genes & Development 29(19):1998-2003. doi: 10.1101/gad.266486.115.

Appendix

List of Figures

Figure 1 Types of POLIII-genes

Figure 2 Y RNA structure

Figure 3 Y RNA conservation

Figure 4 The human Y RNA cluster

Figure 5 Murine Y RNA expression

Figure 6 Y RNA depletion in mice

Figure 7 The 3'-end processing of human Y RNAs

Figure 8 Expression of Y3**

Figure 9 Subcellular localization of Y RNAs

Figure 10 Identification of Y RNA-associated proteins

Figure 11 Y RNA-binding by Ro60

Figure 12 Characterization of Y RNPs

Figure 13 Y RNAs associate with processing factors

Figure 14 Characterization of the Y RNA-CPSF association

Figure 15 The impact of Y RNA depletion on cell growth

Figure 16 The influence of Y RNA depletion on pre-mRNA processing.

Figure 17 Transcriptome wide analysis of mRNA processing

Figure 18 Conservation of the Y3 function

Figure 19 The role of Y3** in histone mRNA processing

Figure 20 The association of Y3** with histone RNAs

Figure 21 Influence of ncRNAs and processing factors on HLB morphology

Figure 22 HLB morphology and dynamics

Figure 23 Proposed model of Y3**'s role in histone mRNA 3'-end processing

List of Tables

Table 1 Ro60 and Y RNA homologs identified in the three domains of life

Abbreviations

ANA	Antinuclear antibody
ASO	Chimeric antisense oligonucleotide
BRF1/2	B - related factor 1/2
CDK	Cyclin-dependent kinase
cDNA	Complementary DNA
CFIm	Mammalian cleavage factor 1
ChIP	Chromatin immunoprecipitation
CPSF	Cleavage and polyadenylation specificity factor
CSTF	Cleavage stimulation factor
DNA	Deoxyribonucleic acid
DSE	Distal/Downstream sequence element
dsRNA	Double-stranded RNA
ER	Endoplasmic reticulum
EZH2	Enhancer of zeste 2 polycomb repressive complex 2 subunit
FLASH	FLICE-associated huge
FRAP	Fluorescence recovery after photobleaching
HEAT-repeat	Domain in huntingtin, elongation factor 3, protein phosphatase 2A, TOR1
HLB	Histone locus body
HNRNPK	Heterogeneous nuclear ribonucleoprotein K
HULC	Highly Up-regulated in Liver Cancer
IGF2BP (1, 2, 3)	Insulin-like growth factor 2 mRNA-binding protein (1, 2, 3)
ivt	<i>In vitro</i> transcribed
kDa	Kilo Dalton
KH-domain	HnRNP K homology domain
MALAT1	Metastasis associated lung adenocarcinoma transcript 1
MEPCE	Methylphosphate capping enzyme
miRNA	Micro RNA
mRNA	Messenger RNA
MS	Mass spectrometry
NB	Northern blot
NCL	Nucleolin
ncRNA	Non-coding RNA
NL	Neonatal Lupus
NPAT	Nuclear protein, ataxia-telangiectasia locus
NTD	N-terminal domain

Oct-1	Octamer-binding transcription factor-1
PAS	Polyadenylation signal
PC	Peptide coverage
PCR	Polymerase chain reaction
PDIA4	Protein disulfide isomerase family A, member 4
piRNA	Piwi-interacting RNA
PNC	Perinucleolar compartment
POLII/III	RNA polymerase II/III
pre-miRNA	Precursor miRNA
PSE	Proximal sequence element
PSM	Peptide spectral matches
PTBP1	Polypyrimidine tract binding protein 1
P-TEFb	Positive transcription elongation factor
PUF60	Poly(U)-binding-splicing factor 60 kDa
qRT-PCR	Quantitative real time PCR
RACE	Rapid amplification of cDNA ends
RBP	RNA-binding protein
RISC	RNA-induced silencing complex
RNA	Ribonucleic acid
RNAi	RNA interference
RNP	Ribonucleoprotein particle
RPL5	60S ribosomal protein L5
RRM	RNA recognition motif
rRNA	Ribosomal RNA
siRNA	Small interfering RNA
SLBP	Stem-loop binding protein
SLE	Systemic lupus erythematosus
SNAPc	Small nuclear RNA activating complex
SRP	Signal recognition particle
snRNA	Small nuclear RNA
snRNP	Small nuclear RNP
snoRNA	Small nucleolar RNA
SS	Sjögren's syndrome
SSB	Sjogren syndrome antigen B (La)
Staf	Selenocysteine tRNA gene transcription-activating factor
TBE	Tris-borate-EDTA buffer

TBP	TATA box binding protein
TFIIIA/B/C	Transcription factor III A/B/C
TLR	Toll-like Receptor
tRNA	Transfer RNA
USE	Upstream sequence element
UTR	Untranslated region
UV	Ultraviolet
VCL	Vinculin
vWFA	Von Willebrand factor type A
WB	Western blot
wt	Wild type
XIST	X-inactive specific transcript
XPO5	Exportin 5

Publications (first author)

1. **Köhn M.**, Lederer M., Wächter K., Hüttelmaier S. (2010)
Near-infrared (NIR) dye-labeled RNAs identify binding of ZBP1 to the noncoding Y3-RNA.
RNA 16(7):1420-8. doi: 10.1261/rna.2152710.
2. **Köhn M.**, Pazaitis N., Hüttelmaier S. (2013)
Why Y RNAs? About Versatile RNAs and Their Functions.
Biomolecules 3(1):143-56. doi: 10.3390/biom3010143.
3. Wächter K.*, **Köhn M.***, Stöhr N., Hüttelmaier S. (2013)
Subcellular localization and RNP formation of IGF2BPs (IGF2 mRNA-binding proteins) is modulated by distinct RNA-binding domains.
Biological Chemistry 394(8):1077-90. doi: 10.1515/hsz-2013-0111.
* shared first authorship
4. **Köhn M.**, Ihling C., Sinz A., Krohn K., Hüttelmaier S. (submitted 2015)
The Y3** ncRNA promotes the 3'-end processing of canonical histone mRNAs.
Submitted to *Genes & Development*

Further publications

1. Weidensdorfer D., Stöhr N., Baude A., Lederer M., **Köhn M.**, Schierhorn A., Buchmeier S., Wahle E., Hüttelmaier S. (2009)
Control of c-myc mRNA stability by IGF2BP1-associated cytoplasmic RNPs.
RNA 15(1):104-15. doi: 10.1261/rna.1175909.
2. Stöhr N., **Köhn M.**, Lederer M., Glass M., Reinke C., Singer R.H., Hüttelmaier S. (2012)
IGF2BP1 promotes cell migration by regulating MK5 and PTEN signaling.
Genes & Development 26(2):176-89. doi: 10.1101/gad.177642.111.
3. Bell J.L., Wächter K., Mühleck B., Pazaitis N., **Köhn M.**, Lederer M., Hüttelmaier S. (2013)
Insulin-like growth factor 2 mRNA-binding proteins (IGF2BPs): post-transcriptional drivers of cancer progression?
Cellular and Molecular Life Sciences 70(15):2657-75. doi: 10.1007/s00018-012-1186-z.

Darlegung des Eigenanteils

1. Köhn M., Lederer M., Wächter K., Hüttelmaier S. (2010)
Near-infrared (NIR) dye-labeled RNAs identify binding of ZBP1 to the noncoding Y3-RNA.
RNA 16(7):1420-8. doi: 10.1261/rna.2152710.
Eigenanteil: Planung, Durchführung und Auswertung aller Experimente. Anfertigung der Figuren und zusammen mit S. H. Anfertigung des Manuskripts. M. L. führte die initiale Aufreinigung des rekombinanten MBP-MS2BP durch. K. W. optimierte die Aufreinigung von NIR-dye markierten RNAs.
2. Köhn M., Pazaitis N., Hüttelmaier S. (2013)
Why Y RNAs? About Versatile RNAs and Their Functions.
Biomolecules 3(1):143-56. doi: 10.3390/biom3010143.
Eigenanteil: Planung, Durchführung und Auswertung des Experiments (Figur 3). Anfertigung der Figuren und zusammen mit S. H. Anfertigung des Manuskripts. N. P. half bei der Isolation von totaler RNA aus Mausgeweben (Figur 3) und bei der Gestaltung der Figuren.
3. Wächter K.*, Köhn M.*, Stöhr N., Hüttelmaier S. (2013)
Subcellular localization and RNP formation of IGF2BPs (IGF2 mRNA-binding proteins) is modulated by distinct RNA-binding domains.
Biological Chemistry 394(8):1077-90. doi: 10.1515/hsz-2013-0111.
* shared first authorship
Eigenanteil: Planung, Durchführung und Auswertung der Experimente (Figur 3B, 3C, 3D, 5C und S1). Anfertigung der entsprechenden Figuren und zusammen mit S. H. und K. W. Anfertigung des Manuskripts. Wichtige Vorarbeiten dieses Manuskripts waren Daten, welche im Zuge der Diplomarbeit von M. K. erzeugt wurden (Lokalisierung und RNA-bindung von ZBP1-Mutanten; Charakterisierung funktioneller Domänen des RNA-bindenden Zipcode Binding Protein 1 (ZBP1), 2008). K. W. führte alle weiteren Experimente durch und erstellte die entsprechenden Figuren. N. S. fertigte die Aufnahmen für Figur 7 an.
4. Köhn M., Ihling C., Sinz A., Krohn K., Hüttelmaier S. (submitted 2015)
The Y3** ncRNA promotes the 3'-end processing of canonical histone mRNAs.
Submitted to *Genes & Development*
Eigenanteil: Planung, Durchführung und Auswertung aller Experimente. Anfertigung der Figuren und zusammen mit S. H. Anfertigung des Manuskripts. C. I. und A. S. führten die MS-Analysen durch (Table S1). K. K. führte die RNA-Sequenzierung inklusive der *library*-Präparationen durch.

Eidesstattliche Erklärung

Hiermit erkläre ich, dass ich meine Dissertationsschrift selbständig und ohne fremde Hilfe verfasst habe. Ich habe keine anderen als die von mir angegebenen Quellen und Hilfsmittel benutzt. Die aus den benutzten Werken wörtlich oder inhaltlich entnommenen Stellen habe ich als solche kenntlich gemacht. Mit der vorliegenden Arbeit bewerbe ich mich erstmals um die Erlangung des Doktorgrades.

Halle (Saale), Juni 2015

Marcel Köhn

Danksagung

Meiner Großmutter Gisela Köhn danke ich für den Rückhalt über die ganzen Jahre hinweg. Sie hat mir ein zu Hause gegeben, mich immer unterstützt und in Allem gefördert, was mir am Herzen lag. Nicht zuletzt hat sie es mir ermöglicht zu studieren und den weiteren wissenschaftlichen Weg einzuschlagen, welcher auch zu dieser Dissertation führte.

Des Weiteren danke ich meiner Tante Beate Köhn und ihrer Familie für ihre unablässige Unterstützung. Bei ihnen fand ich immer einen Ort zum Entspannen und ein Ohr zum Zuhören. Gerade in schweren Zeiten haben wir uns gegenseitig aufgefangen und konnten immer aufeinander zählen.

Professor Stefan Hüttelmaier danke ich für die mittlerweile langjährige wissenschaftliche Zusammenarbeit. Die Diskussionen waren oft inspirierend und haben mich häufig mehr aus meiner Arbeit herausholen lassen, als ich für möglich erachtet hatte. Seine positive Grundeinstellung hat mich so oft aus dem einen oder anderen Tief geholt und wieder optimistisch blicken lassen. Außerdem hat er mir bei vielen Gelegenheiten geholfen Manuskripte zum erfolgreichen Abschluss zu bringen, ungeachtet ob es sich um Anträge, Seminare, Manuskripte, Bewerbungen oder Ähnliches handelte. Die Freiheit in der Forschung erschien mir immer als wichtiger Wert in seiner Arbeitsgruppe. Deshalb möchte ich ihm auch dafür danken, dass er mir die Möglichkeit gab meine wissenschaftlichen Interessen zu verfolgen, auch wenn sie manchmal nicht mit seinen eigenen übereinstimmten. Nicht zuletzt danke ich ihm für die Möglichkeit diese Dissertation bei ihm anfertigen zu dürfen und für seinen Beistand über die Jahre.

Den Mitarbeitern des Hüttelmaier-Labors danke ich für all die Jahre voller fruchtbarer und freundlicher Zusammenarbeit. Ohne euch hätte es mir sicherlich nicht so viel Spaß im Labor gemacht. Gerade die nicht wissenschaftlichen Gespräche haben mein Leben sehr bereichert und etwas Farbe in den Laboralltag gebracht. Sei es nun bei den ‚legendären‘ Weihnachtsfeiern oder einfach nur bei einem Bier am Abend, ihr ward immer für mich da und dafür danke ich euch.

Curriculum Vitae

Vorname: Marcel
 Familienname: Köhn
 Akademischer Grad: Diplom Biochemie
 Geburtsdatum: 04. Januar 1983
 Geburtsort: Wolgast (Deutschland)
 Staatsbürgerschaft: deutsch
 Geschlecht: männlich
 Familienstand: ledig
 Adresse (privat): Adolfstr. 3
 06114 Halle (Saale)
 Adresse (beruflich): Institut für Molekulare Medizin
 Abteilung Molekulare Zellbiologie
 ZAMED - Medizinische Fakultät
 Martin-Luther-Universität Halle-Wittenberg
 Heinrich-Damerow-Str.1
 D-06120 Halle (Saale) Deutschland
 E-Mail: marcel.koehn@medizin.uni-halle.de
 Telefon: (+49)-(0)345-5522873 FAX: -5522894

Fachgebiet der Promotion: Biochemie
 Vorstrafen/Ermittlungsverfahren: Keine

Ausbildung:

Juni 2002: Abitur am Maxim-Gorki-Gymnasium in Seebad Heringsdorf (17424, Deutschland).
 Oktober 2003 – Juni 2008: Studium der Biochemie an der Martin-Luther-Universität Halle-Wittenberg (06108, Deutschland).
 Oktober 2007 – Juni 2008: Diplomarbeit in der Arbeitsgruppe von Prof. Stefan Hüttelmaier an der Martin-Luther-Universität Halle-Wittenberg.
 Titel: Charakterisierung funktioneller Domänen des RNA-bindenden Zipcode Binding Protein 1 (ZBP1).
 Seit August 2008: Promotionsstudent im Labor von Prof. Stefan Hüttelmaier an der Martin-Luther-Universität Halle-Wittenberg. Arbeitstitel: Zelluläre Funktionen von kleinen nicht kodierenden Y-RNAs
 Seit Januar 2015: Position als wissenschaftlicher Koordinator des GRK1591 (DFG)

Halle (Saale), Juni 2015

Marcel Köhn